INTERNATIONAL ATOMIC ENERGY AGENCY
UNITED NATIONS EDUCATIONAL, SCIENTIFIC AND CULTURAL ORGANIZATION
INTERNATIONAL CENTRE FOR THEORETICAL PHYSICS
I.C.T.P., P.O. BOX 586, 34100 TRIESTE, ITALY, CABLE: CENTRATOM TRIESTE

UNITED NATIONS INDUSTRIAL DEVELOPMENT ORGANIZATION

INTERNATIONAL CENTRE FOR SCIENCE AND HIGH TECHNOLOGY
c/o INTERNATIONAL CENTRE FOR THEORETICAL PHYSICS 34100 TRIESTE (ITALY) VIA GRIGNANO, 9 (ADRIATICO PALACE) P.O. BOX 586 TELEPHONE 040-224572 TELEFAX 040-224575 TELEX 460449 APH I

SMR. 628 - 26

Research Workshop in Condensed Matter, Atomic and Molecular Physics (22 June - 11 September 1992)

Working Party on: "Energy Transfer in Interactions with Surfaces and Adsorbates" (31 August - 11 September 1992)

"Charge Exchange in Particle Scattering from Surfaces"

W. HEILAND
Universitat Osnabruck
Fachbereich Physik
Postfach 4469
Barbarastrasse 7
Osnabruck D-4500
GERMANY

These are preliminary lecture notes, intended only for distribution to participants.

Grignano
192

W. Heiland
University of Osnabrück

Charge exchange in particle scattering from surfaces

1) Scattering -- channeling

2) Atomic particles & charge exchange

3) Molecular particles & charge exchange

Plenum Press 1991

Table 1: List of surface analysis techniques

1. Elastic scattering techniques

Acronym	Technique	Probe particle	Det. particle
EELS	Electron energy loss spectr.	Electron	Electron
HREELS	High resolution EELS	Electron	Electron
SEM	Scanning electron microscop	Electron	Electron
ISS (LEIS)	(Low energy) ion scatt. spectr.	Ion	Ion
MEIS	Medium energy ion scattering	Ion	Ion
RBS	Rutherford back scattering	Ion	Ion
ICISS	Impact collision ISS	Ion	Ion
NICISS	Neutral ICISS	Ion	Atom
ERD (DRS)	Elastic recoil detection (Direct recoil sp.)	Ion	Ion
FIM	Field ion microscopy	Atom	Ion

2. Diffraction methods

LEED	Low energy electron diffraction	Electron	Electron
RHEED	Reflection high-energyelectron diffraction	Electron	Electron
HEAD	Helium atom diffraction	Atom	Atom

3. Ionisation methods

AES	Auger electron spectroscopy	Electron	Electron
ÆS	Photoelectron spectroscopy	Photon	Electron
ESCA	Electron spectroscopy for chemical analysis = PES.	Photon	Electron
UPS	Ultraviolett photoelectron spectroscopy	Photon	Electron
ARUPS	Angular resolved UPS	Photon	Electron
XPS	X-ray photoelectron spectr.	Photon	Electron
SEXAFS	Surface extended X-ray absorption fine structure	Photon	Electron
NEXAFS	Near edge X-ray absorption fine structure	Photon	Electron
FEM	Field electron microscopy	Field	Electron

4. Bond breaking

PSD	Photon stimulated desorption	Photon	Ion
ESD	Electron stimulated desorption	Electron	Ion
ESDIAD	ESD ion angular distribution	Electron	Ion
SIMS	Secondary ion mass spectrom.	Ion	Ion
SNMS	Secondary neutral mass spectr.	Ion	Atom
FABS	Fast atom bombardement spec.	Atom	Atom
ERD	Elastic recoil detection (Direction recoil sp.)	Ion	Ion

5. Charge exchange methods

INS	Ion neutralisation spectr.	Ion	Electron
MDS	Metastable de-excitation spectr.	Atom	Electron
STM	Scanning tunneling microscopy	(tip)	Electron

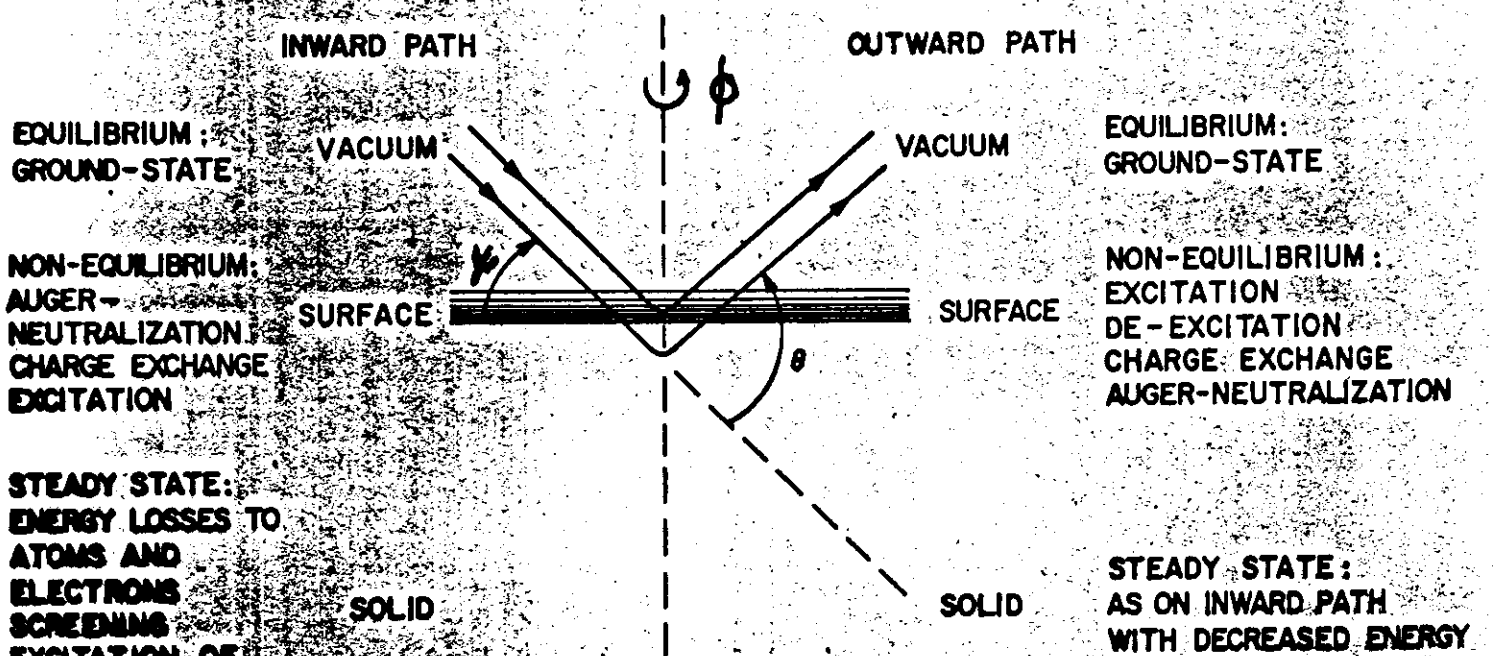
INWARD PATH
OUTWARD PATH
EQUILIBRIUM ;
GROUND-STATE
VACUUM
VACUUM
EQUILIBRIUM:
GROUND-STATE
NON-EQUILIBRIUM:
AUGER-
NEUTRALIZATION
CHARGE EXCHANGE
EXCITATION
SURFACE
SURFACE
NON-EQUILIBRIUM:
EXCITATION
DE-EXCITATION
CHARGE EXCHANGE
AUGER-NEUTRALIZATION
STEADY STATE:
ENERGY LOSSES TO
ATOMS AND
ELECTRONS
SCREENING
EXCITATION OF
PHONONS,
PLASMONS,
RADIATION DAMAGE
SOLID
SOLID
STEADY STATE:
AS ON INWARD PATH
WITH DECREASED ENERGY

D. P. Jackson

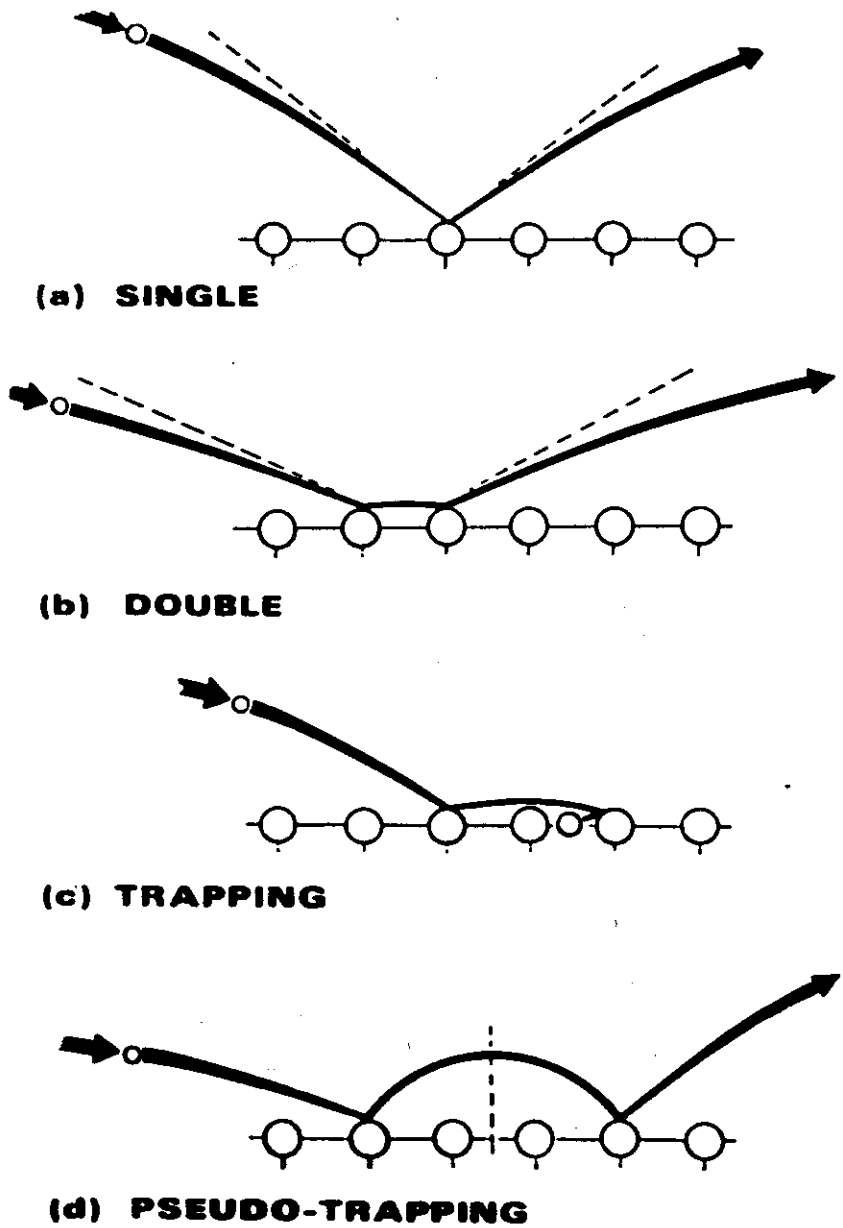

Fig. 9. Some trajectory possibilities seen in gas surface scattering.

Channeling

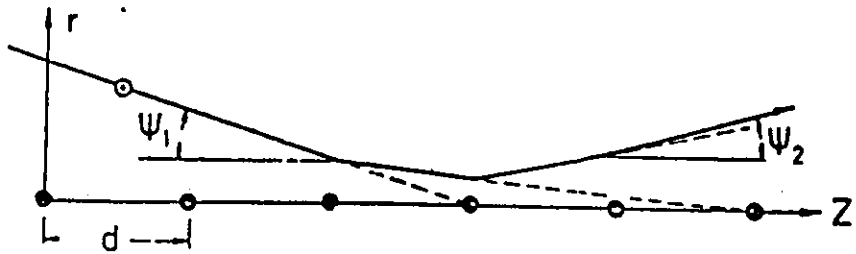

Blocking

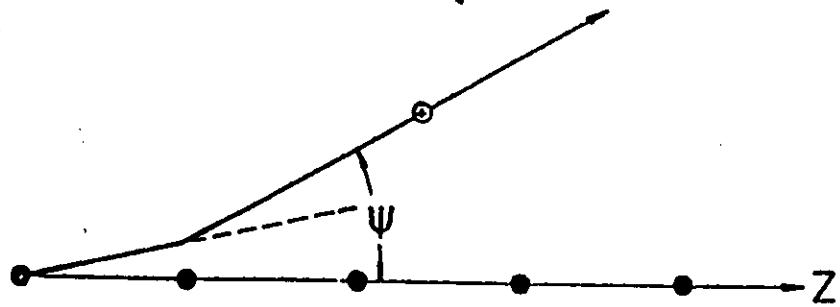

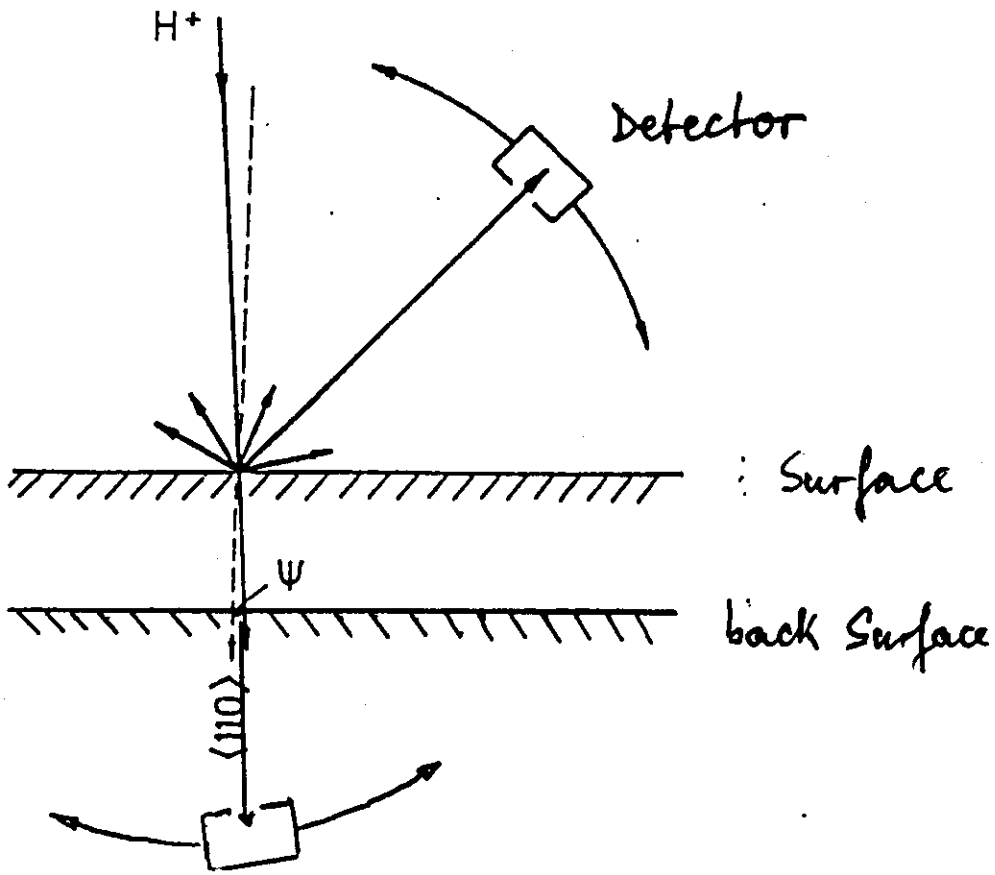

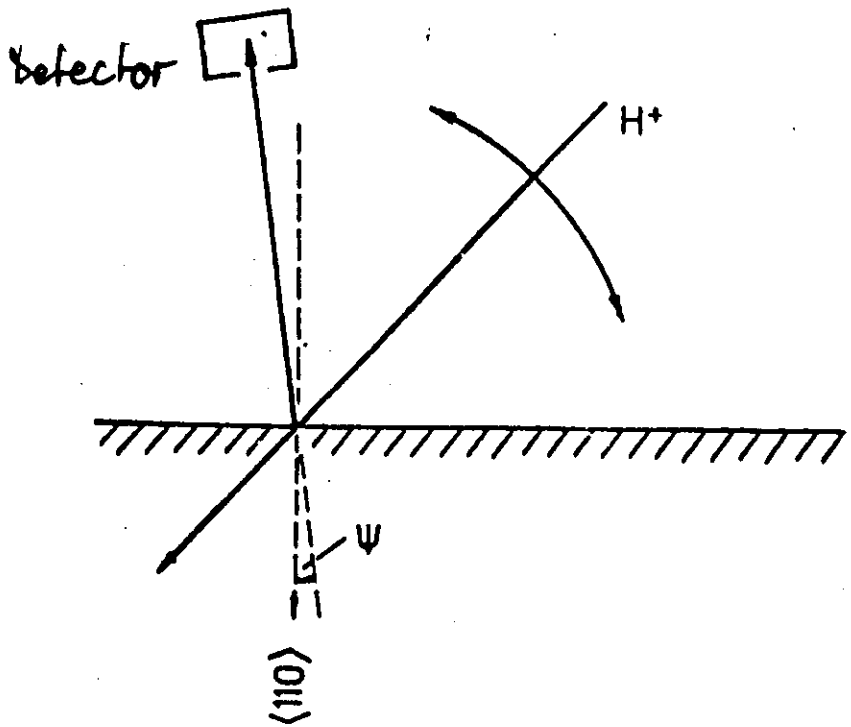

THE CHANNELING OF ENERGETIC ATOMS IN CRYSTAL LATTICES

Mark T. Robinson and O. S. Oen

Solid State Division, Oak Ridge National Laboratory[1]

Oak Ridge, Tennessee

(Received 5 December 1962)

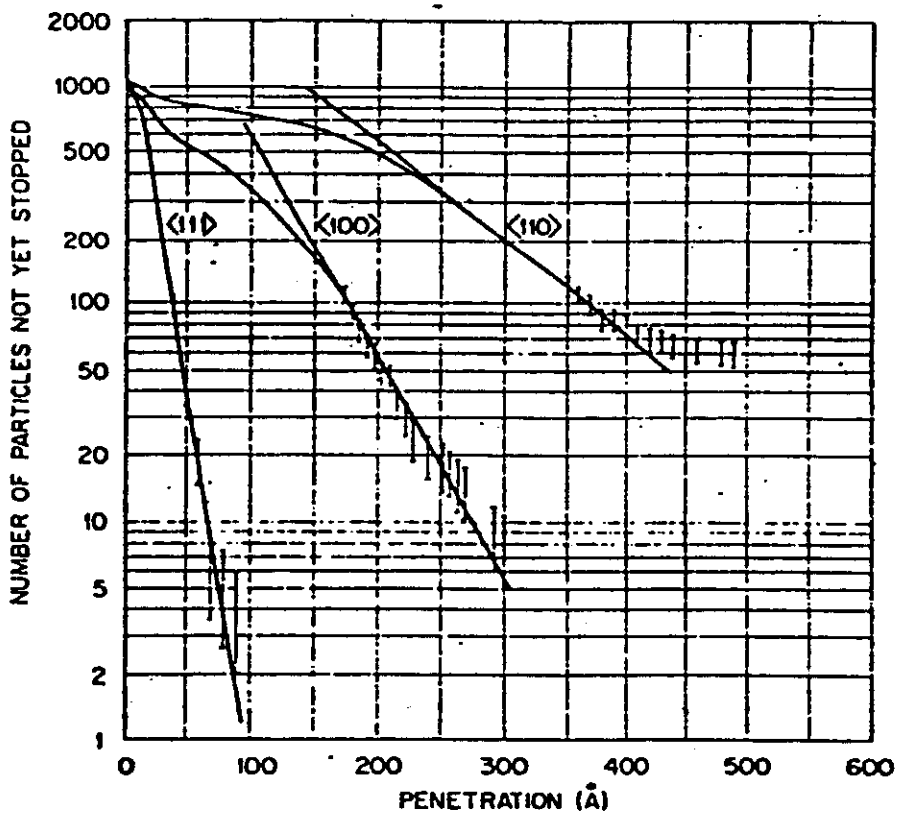

5-kev Cu Atoms Slowing Down in Cu, Born-Mayer Potential; Static Lattice; Initial Directions as Given on Curves.

Fig. 1. Integral penetration distributions calculated for 5-keV Cu atoms slowing down in a static Cu lattice according to the Born-Mayer potential. The initial directions of the incident particles are given on the curves. The vertical bars give estimates of the statistical uncertainties in the calculations in the tail regions.

matematisk-fysiske meddelelser
udgivet af
Det Kongelige Danske Videnskabernes Selskab
Bind 34, nr. 14

Mat. Fys. Medd. Dan. Vid. Selsk. 34, no. 14 (1965)

INFLUENCE OF CRYSTAL LATTICE ON MOTION OF ENERGETIC CHARGED PARTICLES

BY

JENS LINDHARD

Classical Rutherford shadow behind one atom

A simple and illustrative phenomenon is the shadow behind a repul scattering centre in an external, parallel beam of particles. The scatter is assumed to be classical (cf. (B.4) and (B.5)), and we suppose that th is a screen perpendicular to the beam, at a distance d behind the scatte centre. This idealized experiment may be said to represent a pair of at the scattering centre being one atom, the second atom being placed in screen, so that we ask for the probability of hitting the second atom.

An example of nearly isolated atomic pairs is found e.g. for ne neighbours in the diamond lattice, i.e. in the ⟨1 1 1⟩-direction. Such may also be regarded as incomplete strings, with successively two occu and to unoccupied sites. The pair effect can occur not merely in a s atomic substance like Si, but also in e.g. ZnS, where all S atoms are shie by Zn atoms in one direction, and conversely in the opposite directi

For simplicity, we consider merely Rutherford scattering, corresponding to impact parameters $p \leq a$. Let the scattering centre be placed on the z-axis, the beam being parallel to this axis. A particle with impact parameter p hits the screen at a distance r from the z-axis, and for small angles of deflection ϑ is given by

$$r = p + \frac{b}{p} d, \tag{2.11}$$

where $b = Z_1 Z_2 e^2/E$. The distance r has a minimum, $r_{min} = 2\sqrt{bd}$, for $p = \sqrt{bd}$. The shadow region therefore has a parabolic shape, as a function of the distance d, since its edge is at $r = r_{min} \propto d^{1/2}$.

In order to hit the centre of the screen, we must tilt the beam by an angle $\vartheta_{min} = 2\sqrt{b/d} = \vartheta_1/\sqrt{2}$, where ϑ_1 is given by (2.9). The intensity distribution on the screen is easily obtained from (2.11). Let $f(r)$ be the intensity on the screen, the external beam containing one particle per unit area. Then, for large r, $f(r)$ tends to unity, whereas $f(r) = 0$ for $r < r_{min}$. The particles aiming at $r < r_{min}$ are pushed just outside r_{min}, where $f(r)$ has a peak. In fact,

$$f(r) = \begin{cases} 0, & r < r_{min} \\ \frac{1}{2}\left|\left(1 - \frac{r_{min}^2}{r^2}\right)^{1/2} + \left(1 - \frac{r_{min}^2}{r^2}\right)^{-1/2}\right|, & r > r_{min}. \end{cases} \tag{2.12}$$

The sharp edge at $r = r_{min}$ is blurred when quantal corrections are taken into account, the blurring remaining small only when $\varkappa = 2Z_1 Z_2 e_0^2/v$ is large compared to unity (cf. (2.29)).

The number of particles missing on the screen inside r_{min} is πr_{min}^2. The number missing inside r is $\pi r^2 - \int_{r_{min}}^{r} 2\pi r dr f(r) = \pi r^2 (1 - (1 - r_{min}^2/r^2)^{1/2})$. For large r this implies that only half the missing number is compensated in Rutherford scattering with $p \propto d$. It is easy to show that, for screened atomic fields, the full compensation occurs for r larger than a. In fact, when (2.6') holds, a 75 per cent compensation is obtained for $r = Ca$. Thus, for fast particles obeying eq. (2.9') the compensation is divided in two equal parts, one occurring at $r \geq 2(bd)^{1/2}$, or $\vartheta \geq \vartheta_1/\sqrt{2}$, and the other at $r \sim Ca$, or $\vartheta \sim Ca/d$.

Blocking

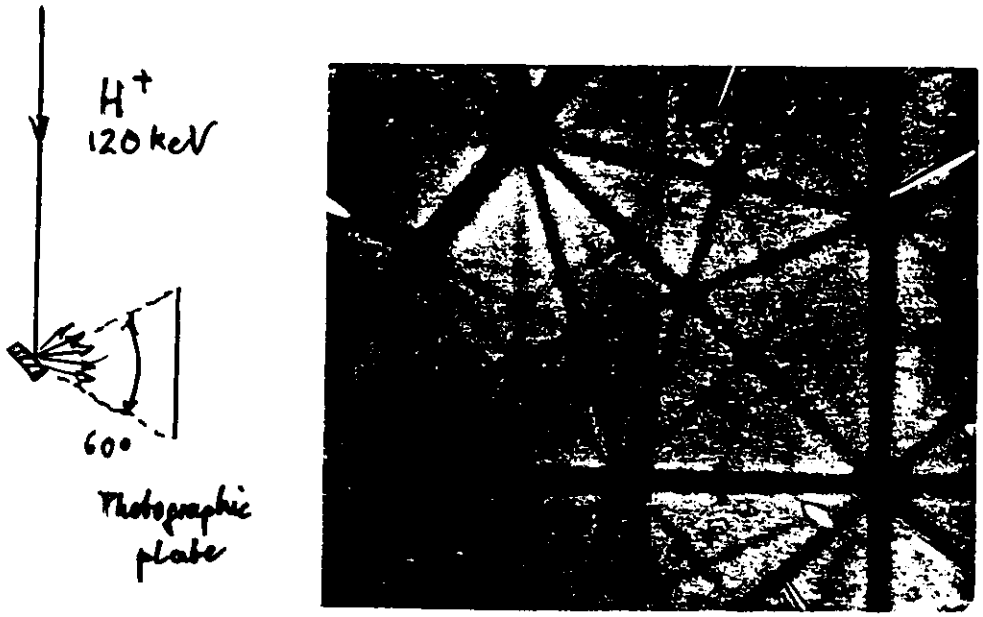

R. Rehrisch
1968

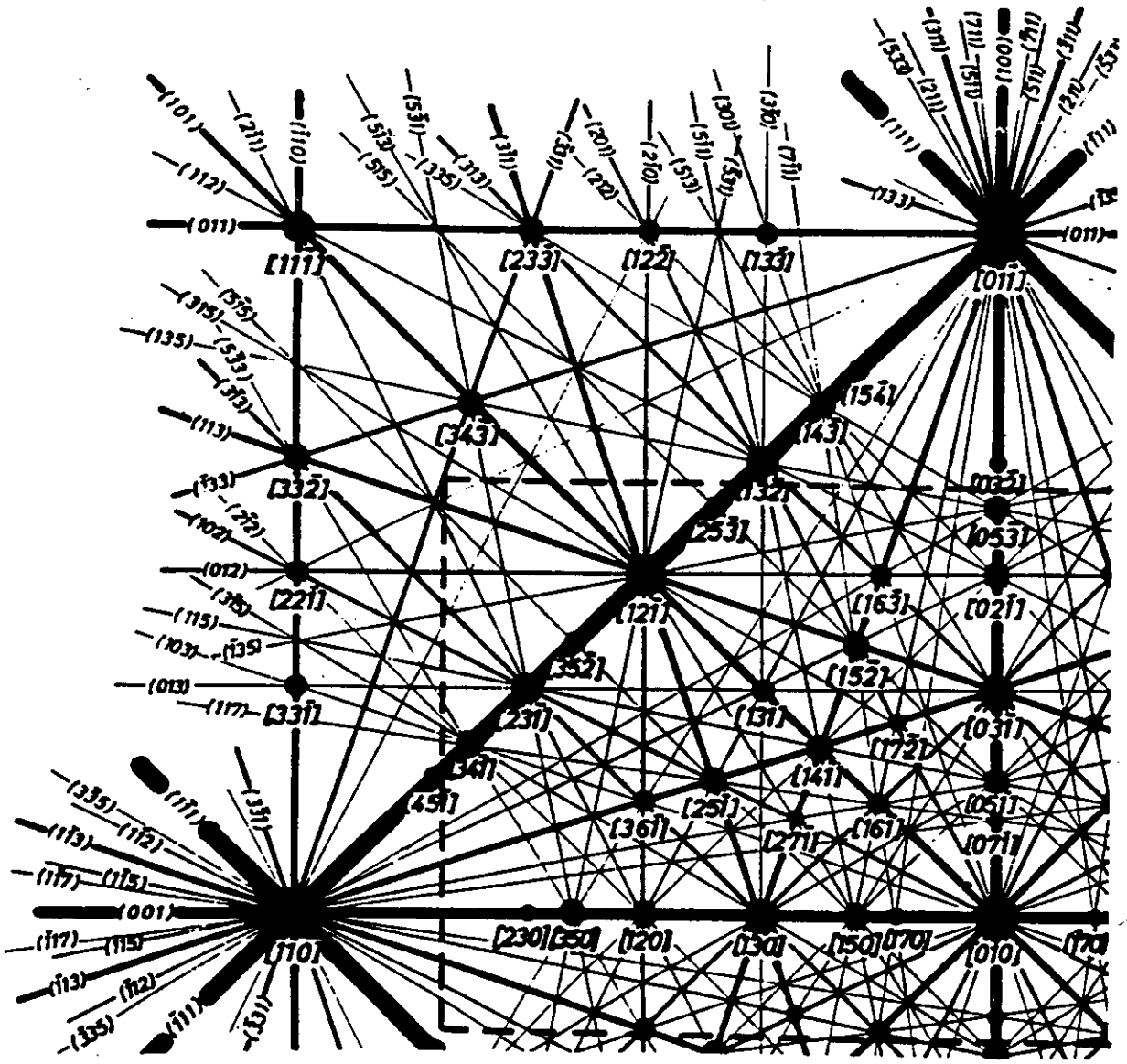

oben: Photographische Aufnahme der von einem Cu-Einkristall zurückgestreuten Wasserstoffatome. E_1 = 120 keV, die Photoplatte war empfindlich für E > 60 keV.
unten: Gnomonische Projektion eines kfz-Gitters in [010]-Richtung. Der Ausschnitt der photographischen Aufnahme ist eingezeichnet.

1976

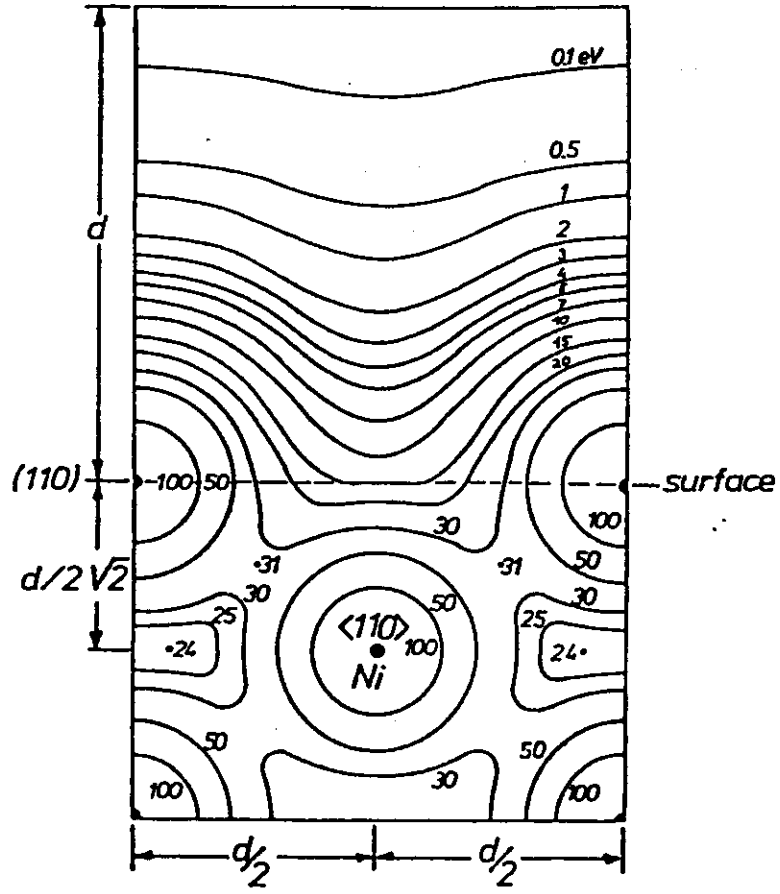
0.1 eV
0.5
1
2
3
4
5
7
10
15
20
d
(110)
100
50
surface
30
100
d/2√2
31
31
50
30
30
25
25
24
24
<110>
100
Ni
50
50
30
100
100
d/2
d/2

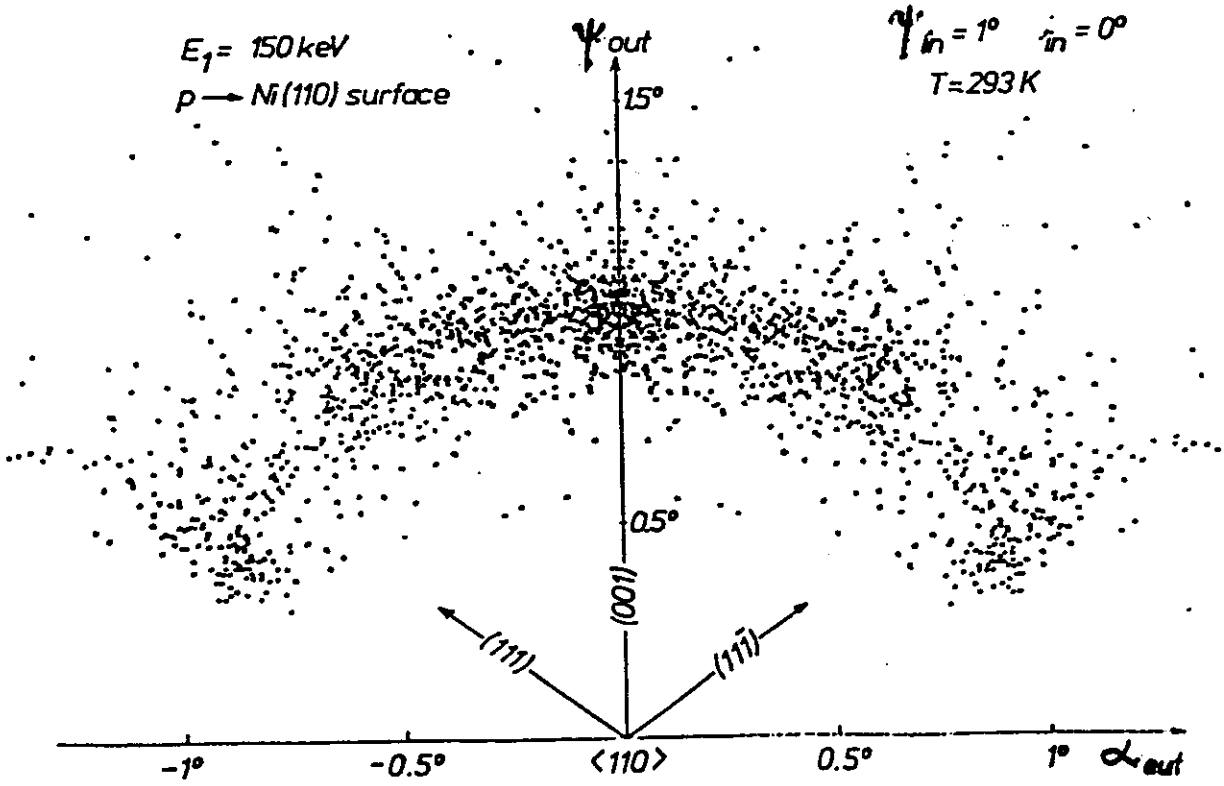
E1 = 150 keV
p → Ni(110) surface
ψout
ψin = 1°
φin = 0°
T = 293 K
1.5°
0.5°
(001)
(111)
(11$\bar{1}$)
-1°
-0.5°
<110>
0.5°
1°
αout

W. Hetterich et al
Surf Sci 1991

90060808 (1×1) CO - Präparation

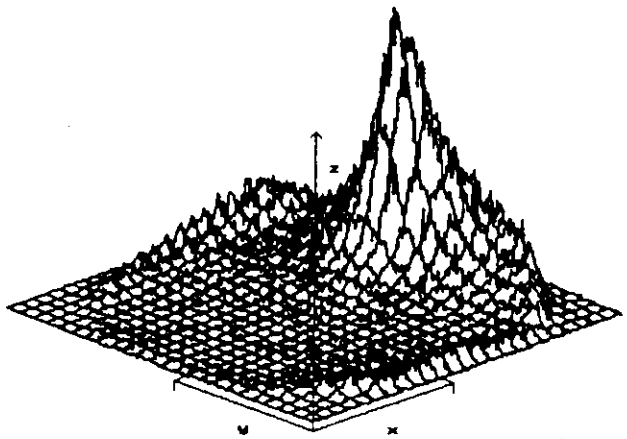

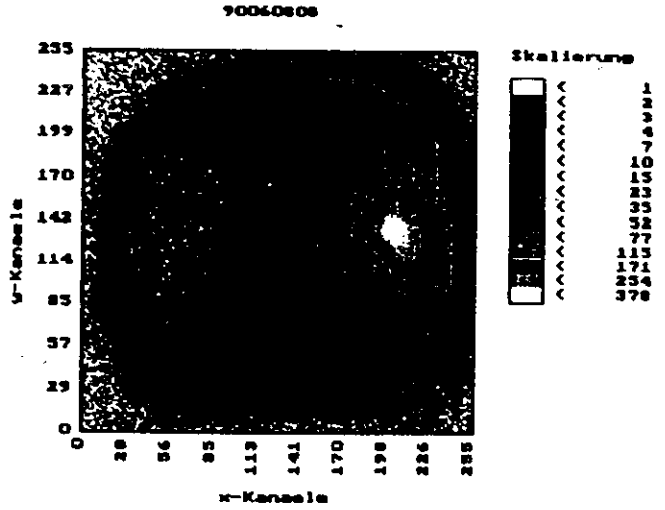

90060806 (1×1) O_2 - Präparation

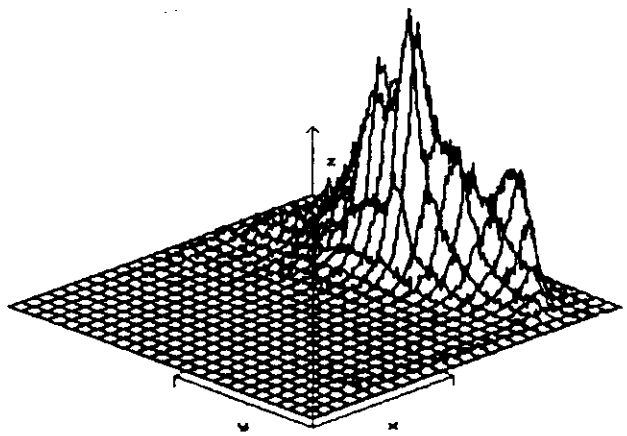

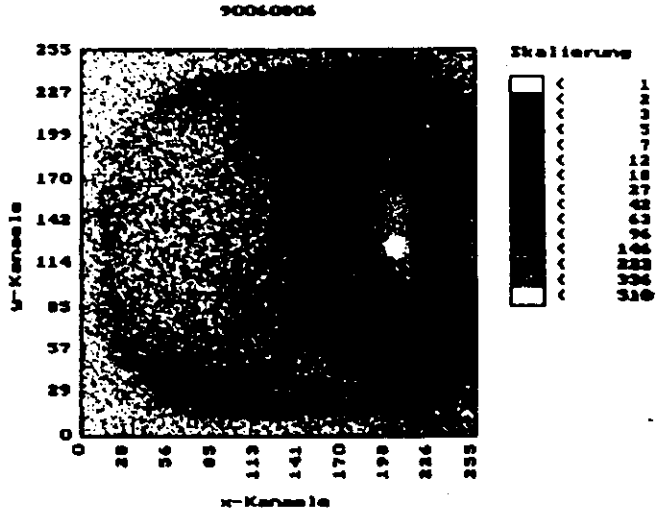

90060804 "(1×3)" nach Tempern

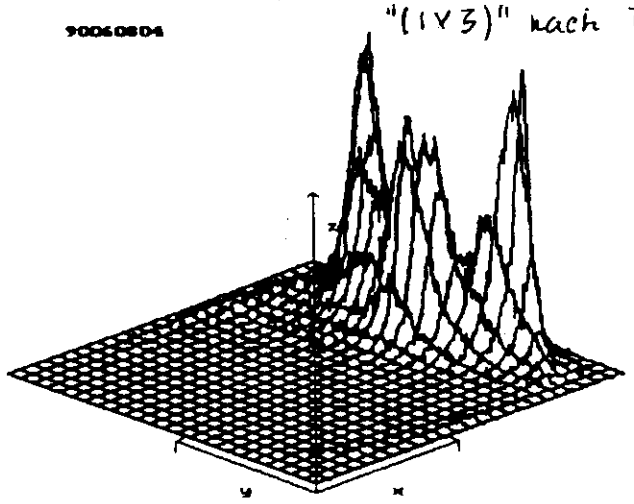

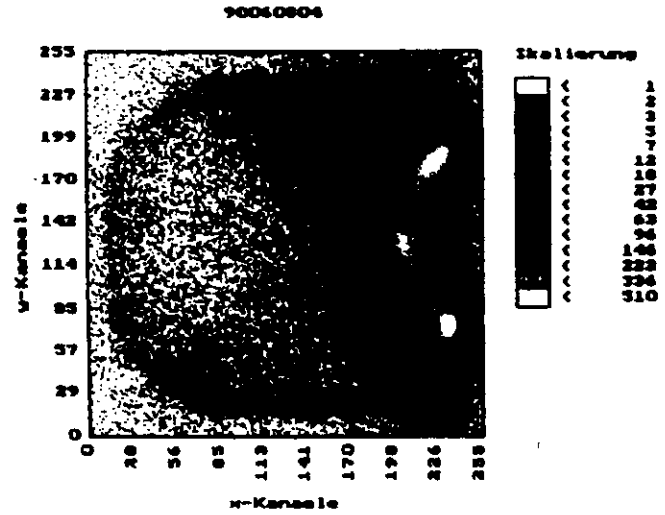

3.5 keV Ne^+, $\psi = 4.5°$

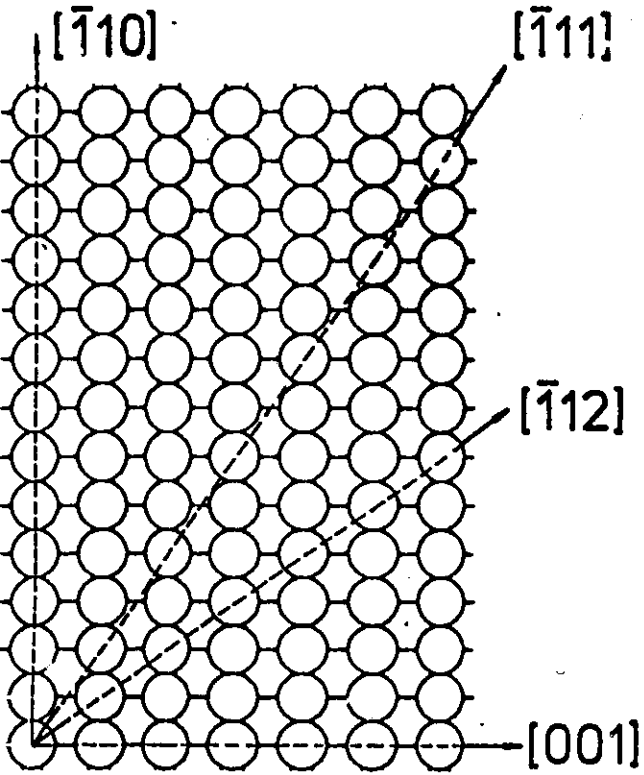
[$\bar{1}$10]
[$\bar{1}$11]
[$\bar{1}$12]
[001]

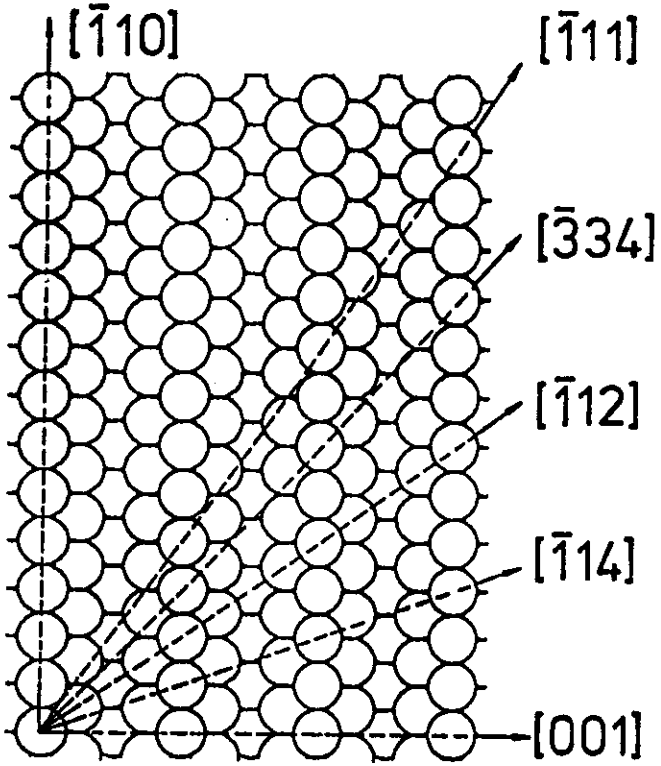
[$\bar{1}$10]
[$\bar{1}$11]
[$\bar{3}$34]
[$\bar{1}$12]
[$\bar{1}$14]
[001]

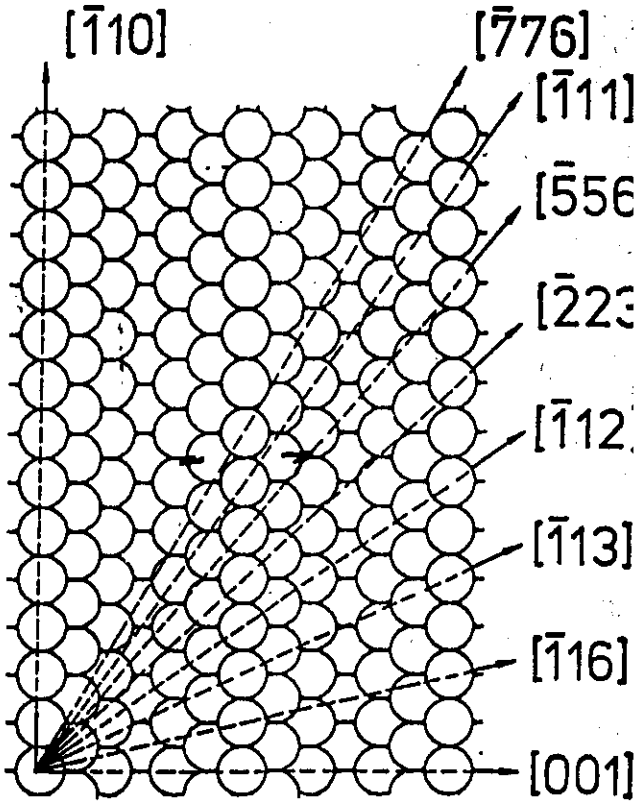
[$\bar{1}$10]
[$\bar{7}$76]
[$\bar{1}$11]
[$\bar{5}$56
[$\bar{2}$23
[$\bar{1}$12
[$\bar{1}$13]
[$\bar{1}$16]
[001]

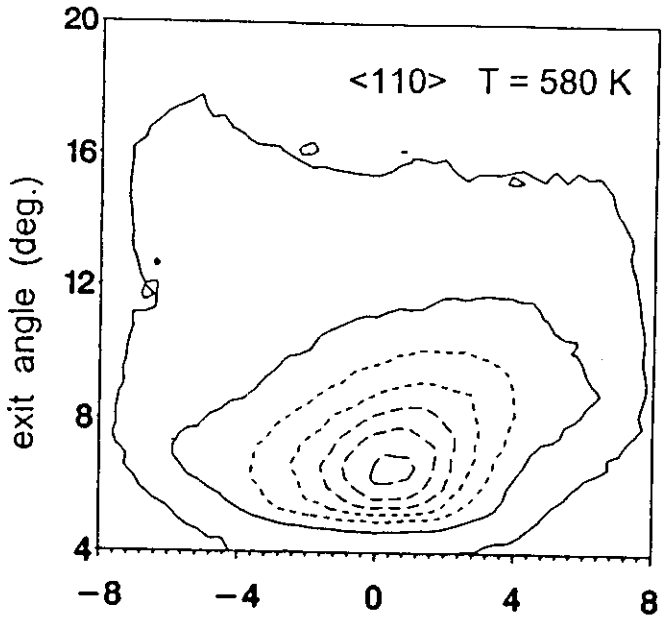
<110> T = 580 K
exit angle (deg.)
20
16
12
8
4
−8
−4
0
4
8

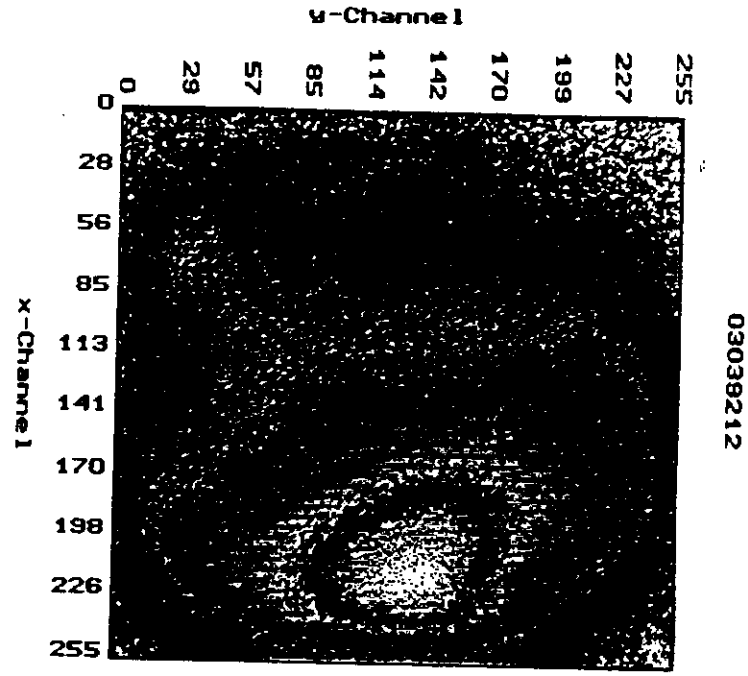
y-Channel
x-Channel
0
28
56
85
113
141
170
198
226
255
29
57
85
114
142
170
199
227
255
03038212

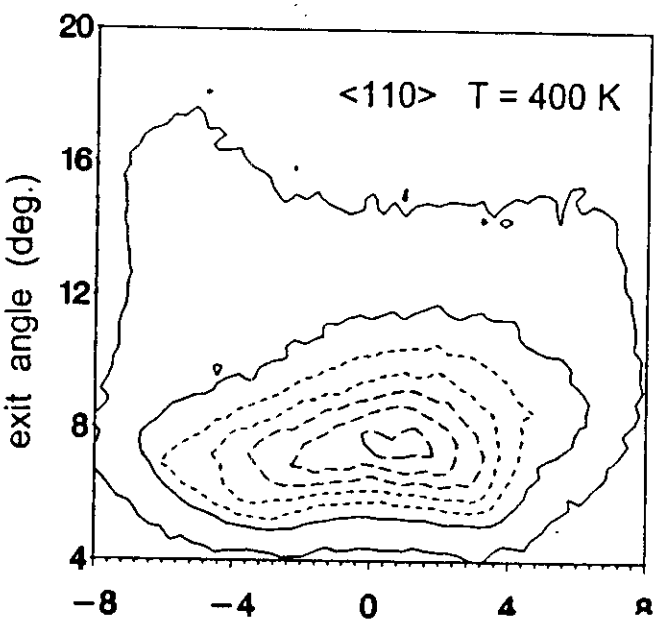
<110> T = 400 K
exit angle (deg.)
20
16
12
8
4
−8
−4
0
4

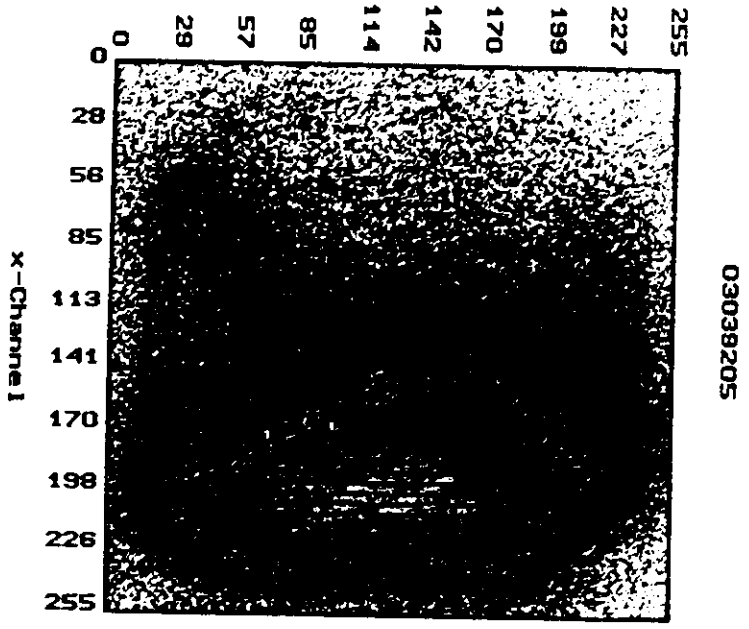
x-Channel
0
28
58
85
113
141
170
198
226
255
29
57
85
114
142
170
199
227
255
03038205

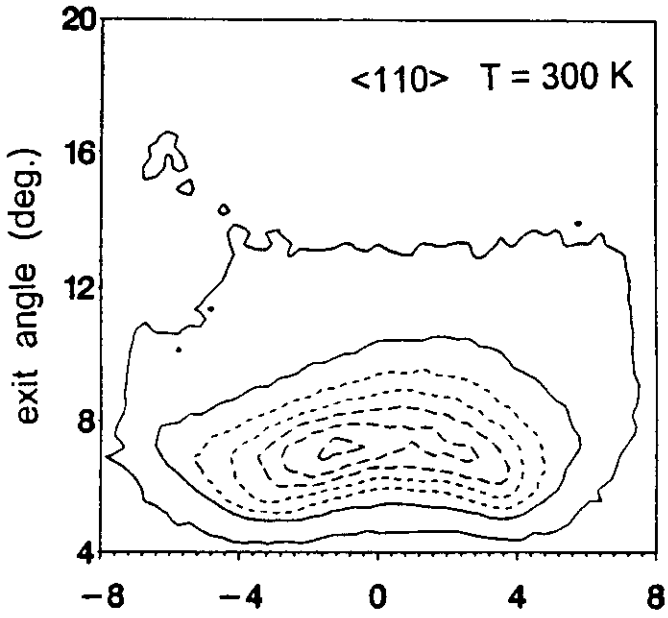
<110> T = 300 K
exit angle (deg.)
20
16
12
8
4
−8
−4
0
4
8

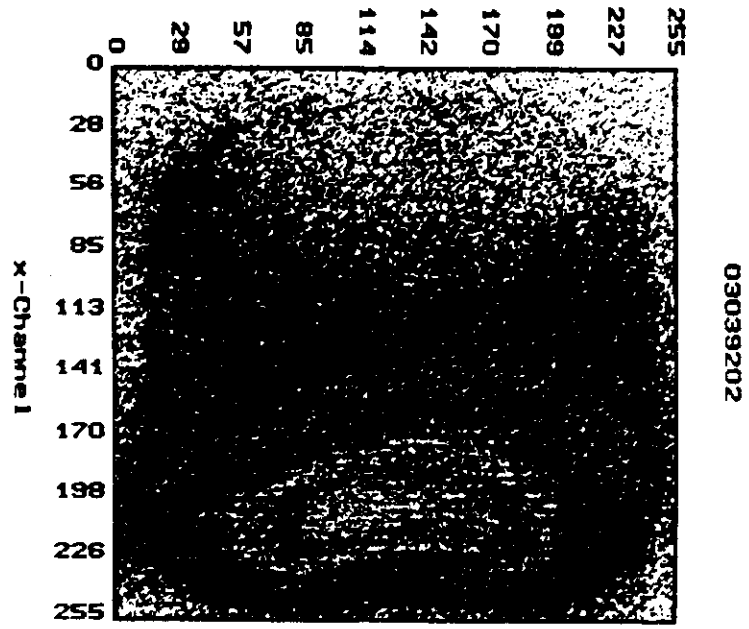
x-Channel
0
28
58
85
113
141
170
198
226
255
29
57
85
114
142
170
199
227
255
03038202

Pb(110)
S. SPELLER
1991
Phys Rev. Lett '92

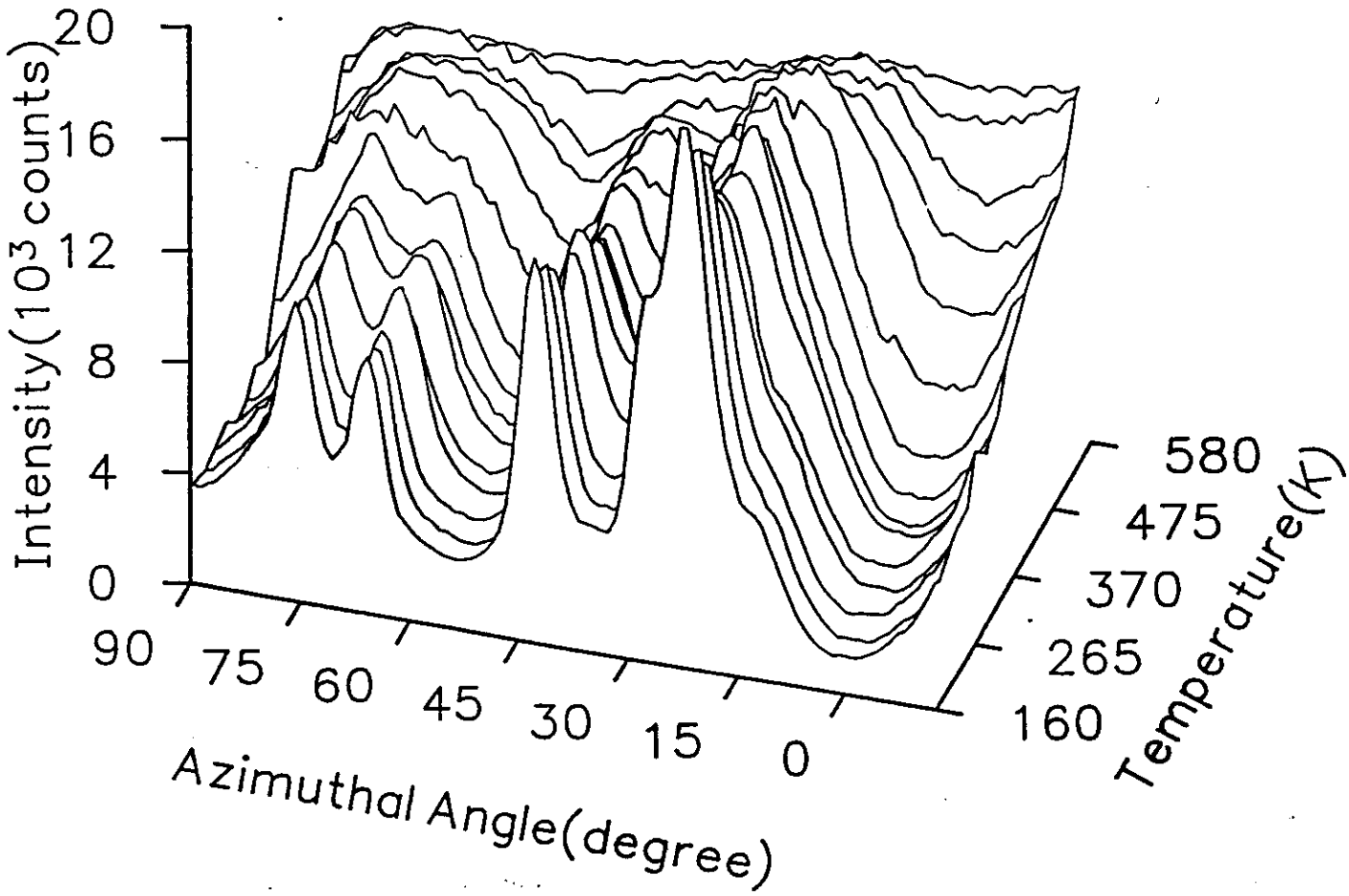

LOKI

Moller et al
Innsbruck

Experimenteller Aufbau

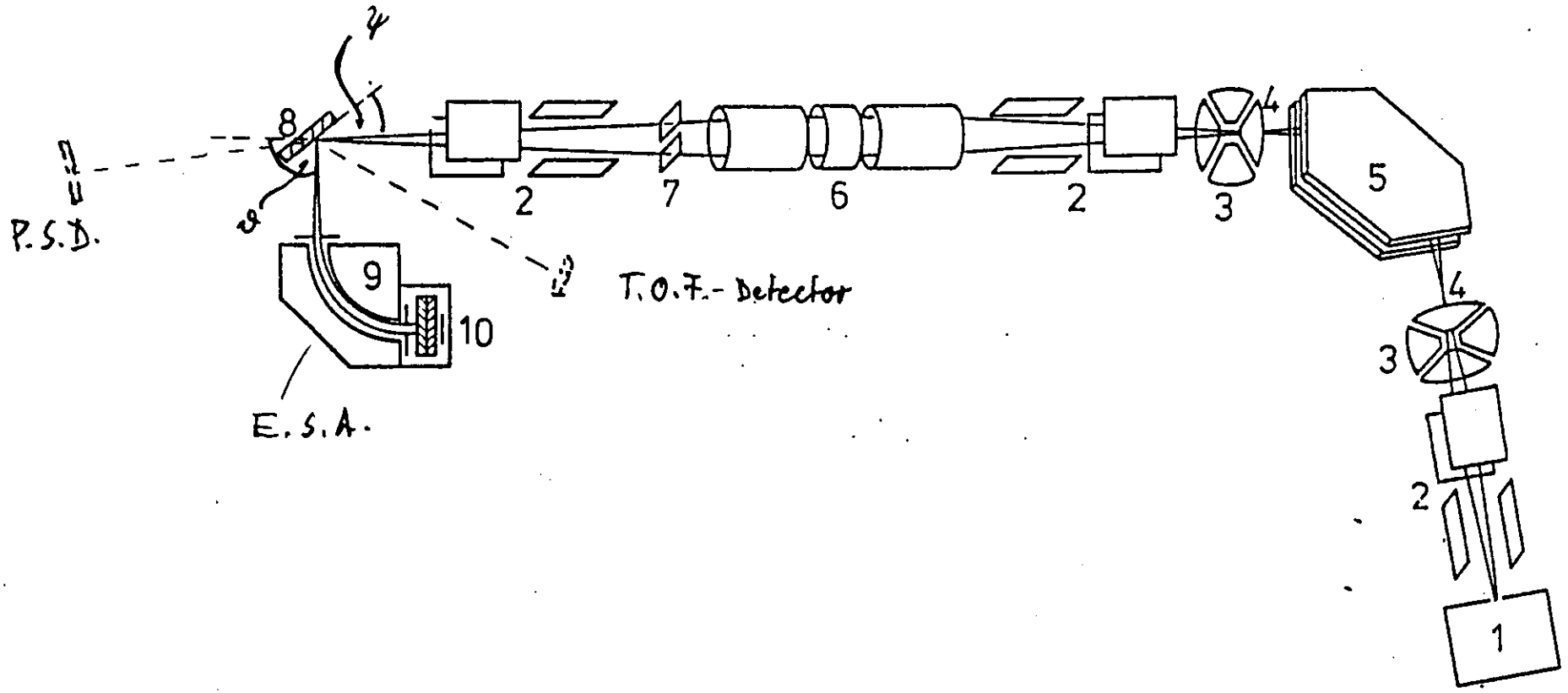

Abb. 2.4: Führungselemente des Ionenstrahls der LLOKI-Apparatur (1) ATOMICA Ionenquelle, (2) Ablenkplatten, (3) segmentierte Blende, (4) Brennpunkt, (5) Magnet, (6) Einzellinse, (7) verstellbarer Spalt, (8) Probe, (9) Analysator, (10) Detektor

H. Betts '89 MARLOWE (M.T. Robinson, D.S. Gem
U. of Oz.

[1 1 $\bar{0}$]

He → Ni(110)

3 keV, $\psi = 5°$, $\vartheta = 10°$

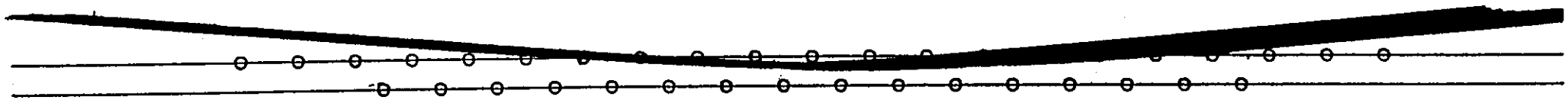

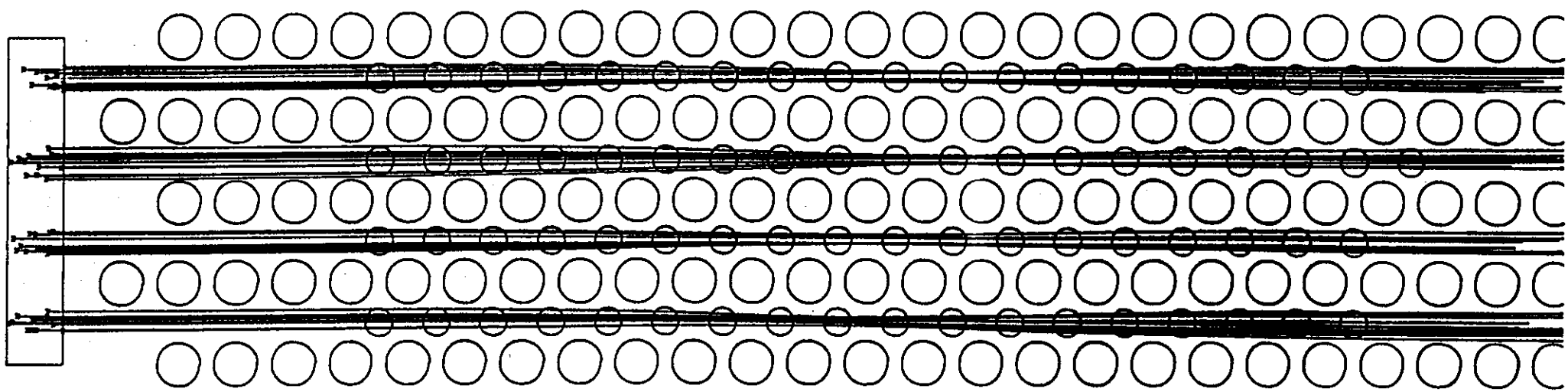

A. Närmann
U. of OS

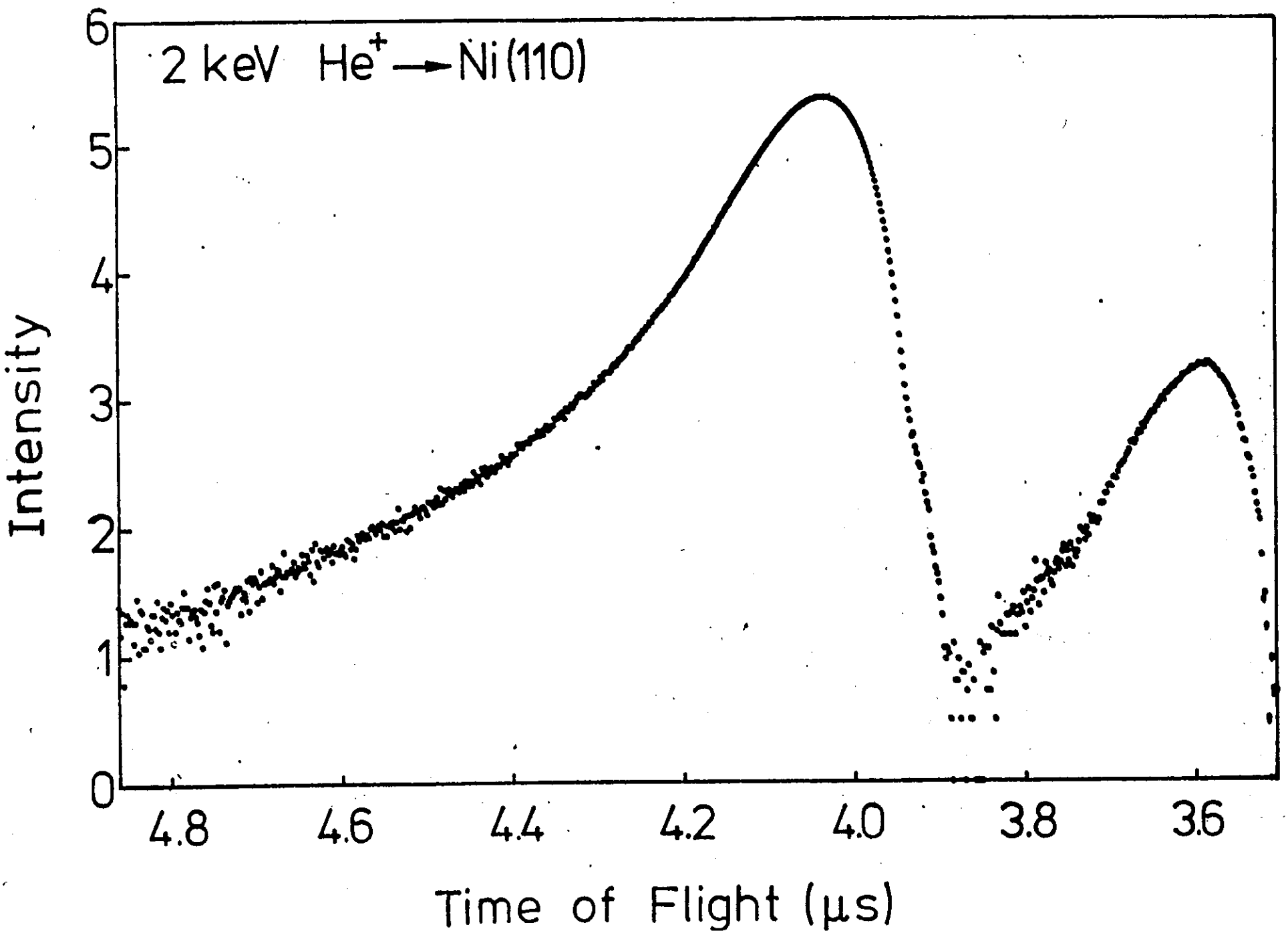

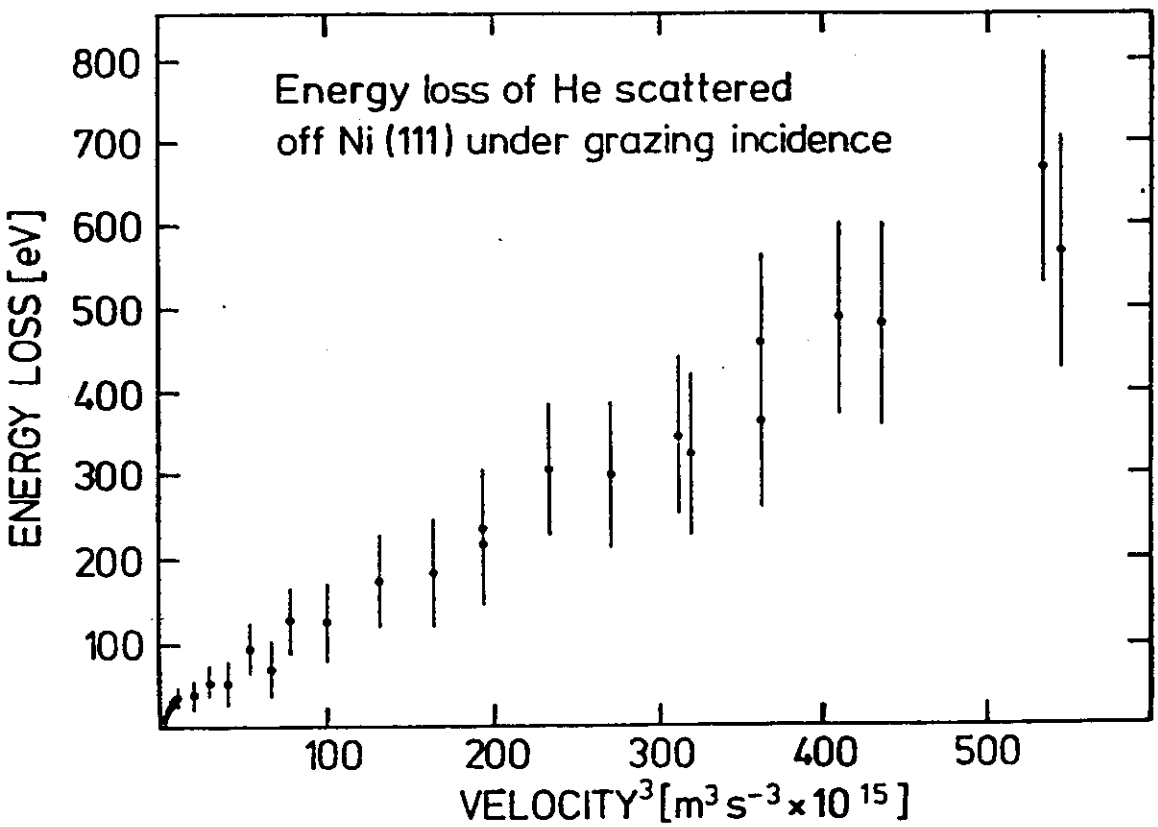
Energy loss of He scattered
off Ni (111) under grazing incidence
ENERGY LOSS [eV]
800
700
600
500
400
300
200
100
100
200
300
400
500
VELOCITY^3 [m^3 s^{-3} × 10^{15}]

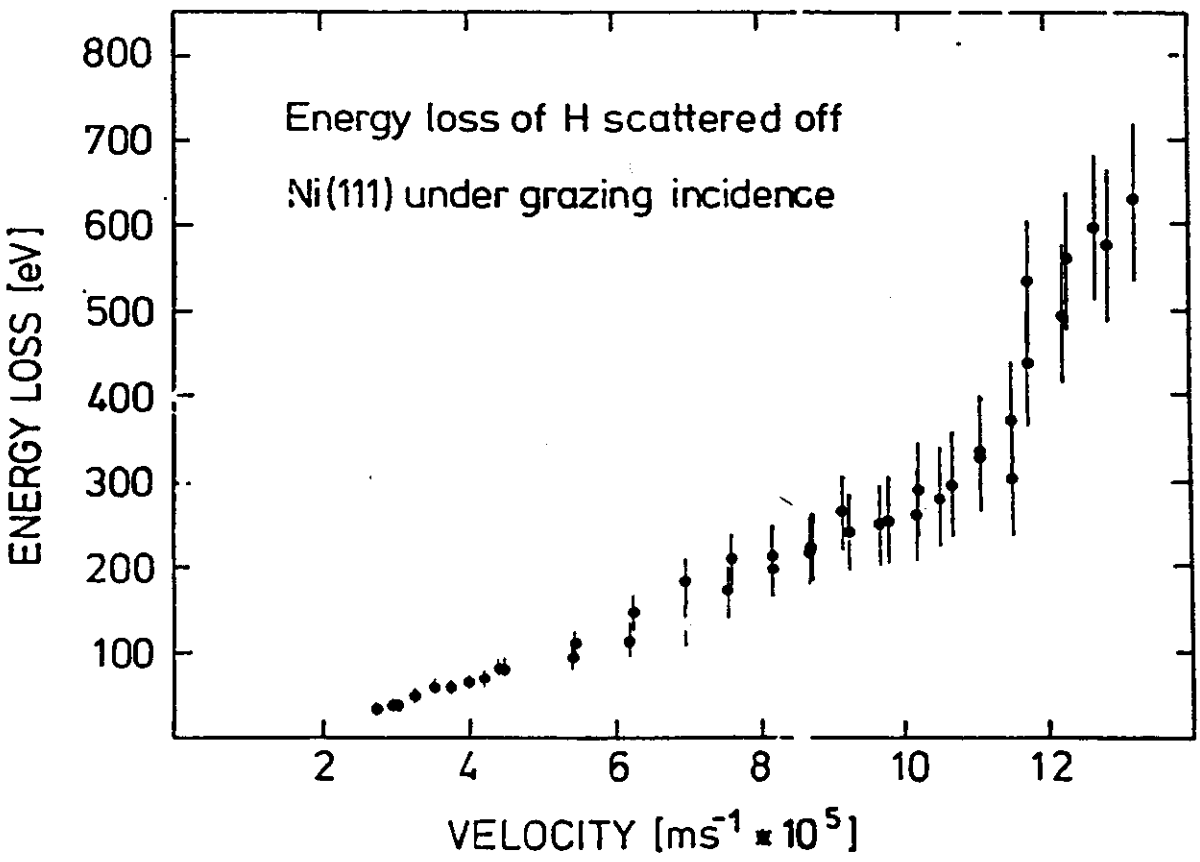
Energy loss of H scattered off
Ni(111) under grazing incidence
ENERGY LOSS [eV]
800
700
600
500
400
300
200
100
2
4
6
8
10
12
VELOCITY [ms^{-1} × 10^5]

Energy Loss of H scattered from Ni at Low Energies.

A. Närmann, H. Fraulke, K. Schmidt, C. Höfner
W. Heiland
Universität Osnabrück

① A. Närmann et al P.R.L. 64 (1990) 1601
Charge exchange and energy dissipation

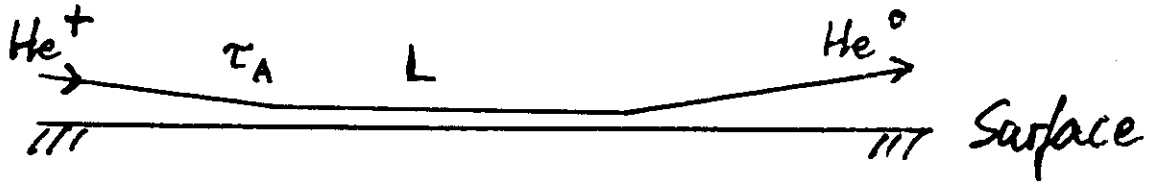

H. Berks et al N.I.M. B 44 (1989) 125 Channeling
R. Monreal et al Surf. Sci. 211/212 (1989) 271 τ_A

$Q_p \sim v^3$ i.e. $Q_p = v \bar{\gamma}_s L$ $\bar{\gamma}_s \propto v$

② $H^+ \longrightarrow$ Surface $\longrightarrow H^0, H^+, H^-$

$Q_p \sim v^n$ $n \simeq 2$ or $\bar{\gamma}_s \propto 1/v$

" H^- "

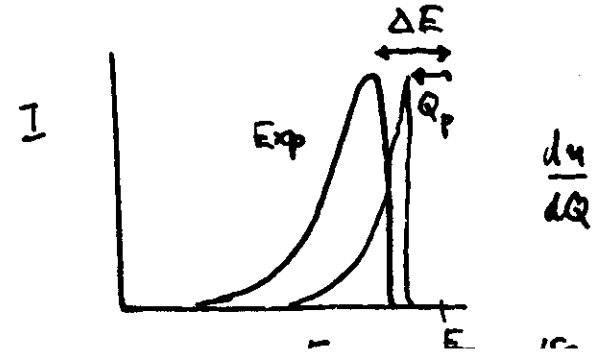

$\frac{dq}{dQ}$ without straggling

A. Närmann et al Phys. Rev. Lett 64 (1990) 1661

Energy distribution + Straggling (3 keV He → Ni)
"Surface Scattering"

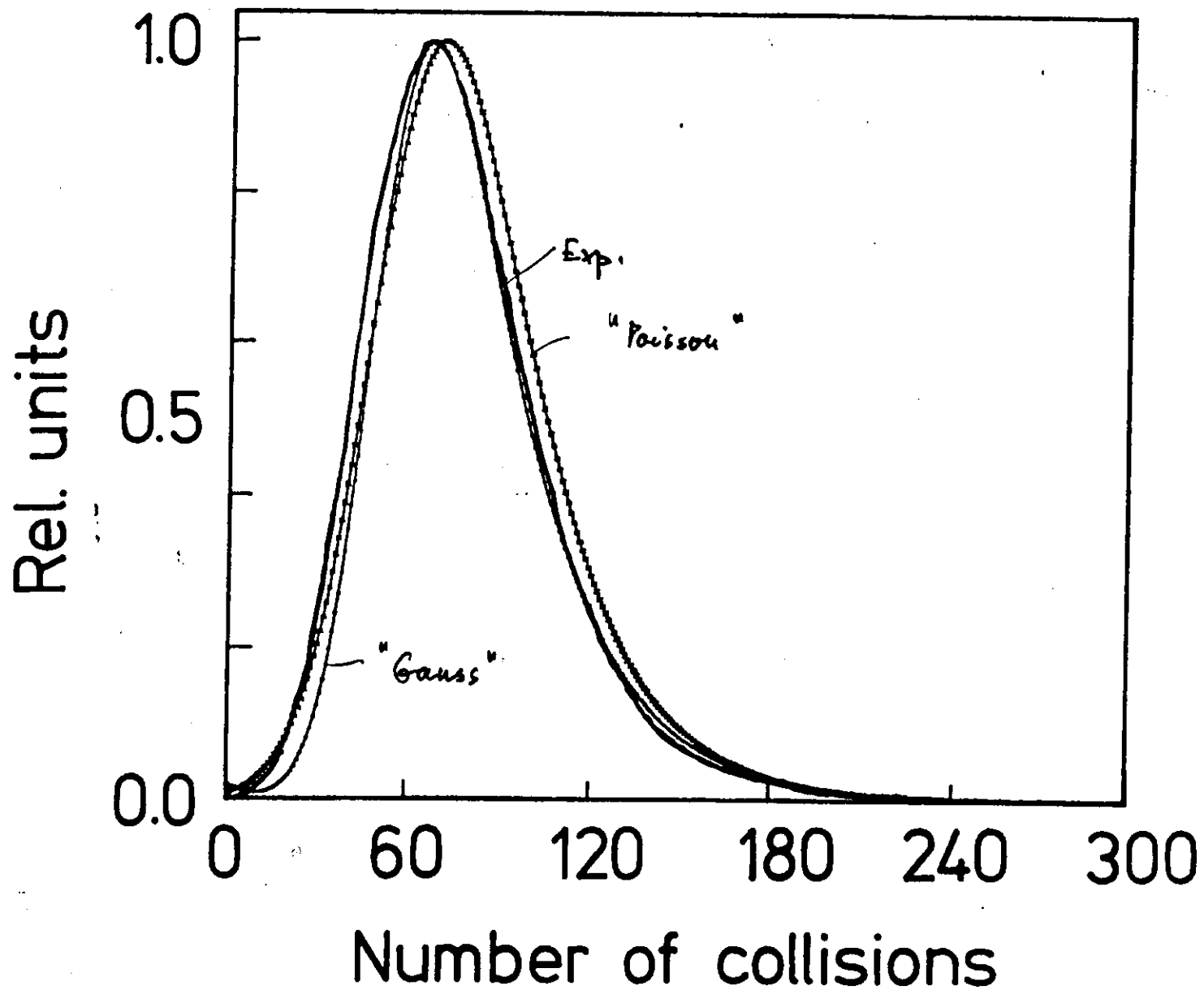

4. DIG

Nucl Instr. Meth '92

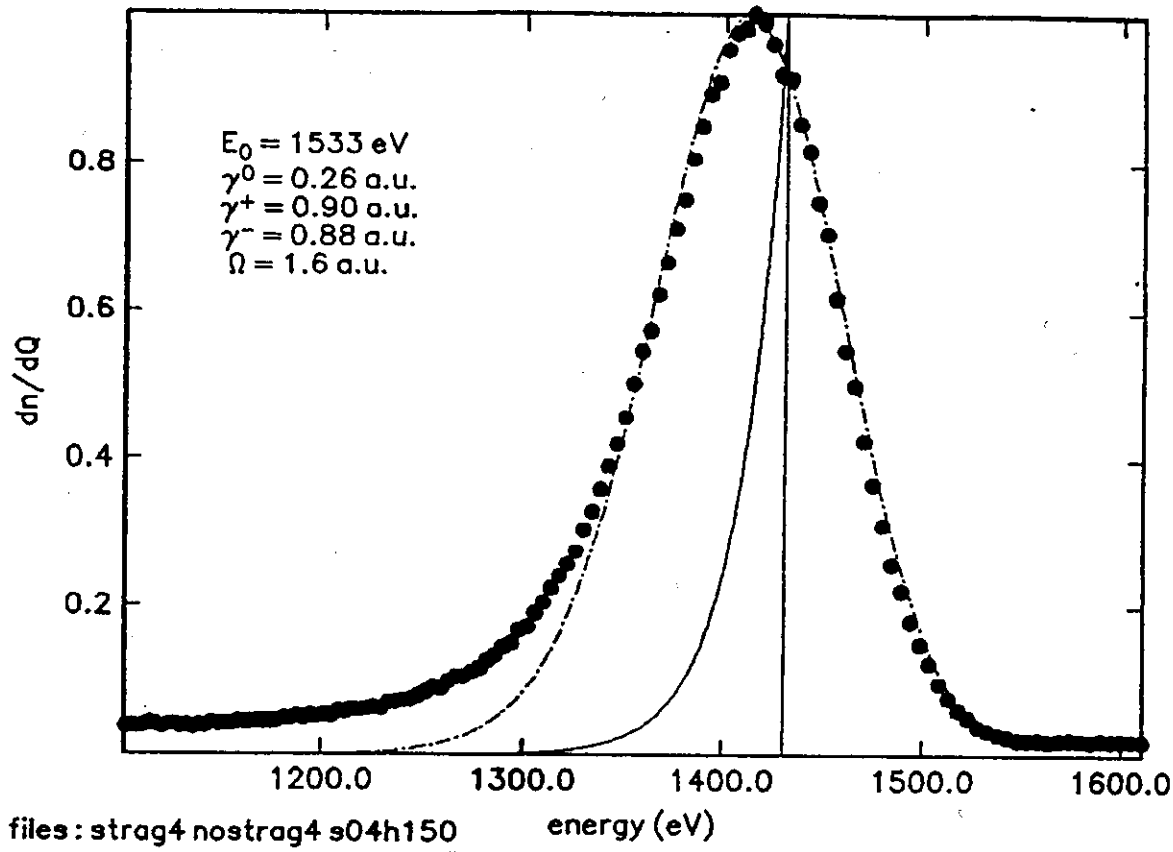

1.533 keV H^+ $\psi = 5°$ $\vartheta = 10°$ [random

5. DIG

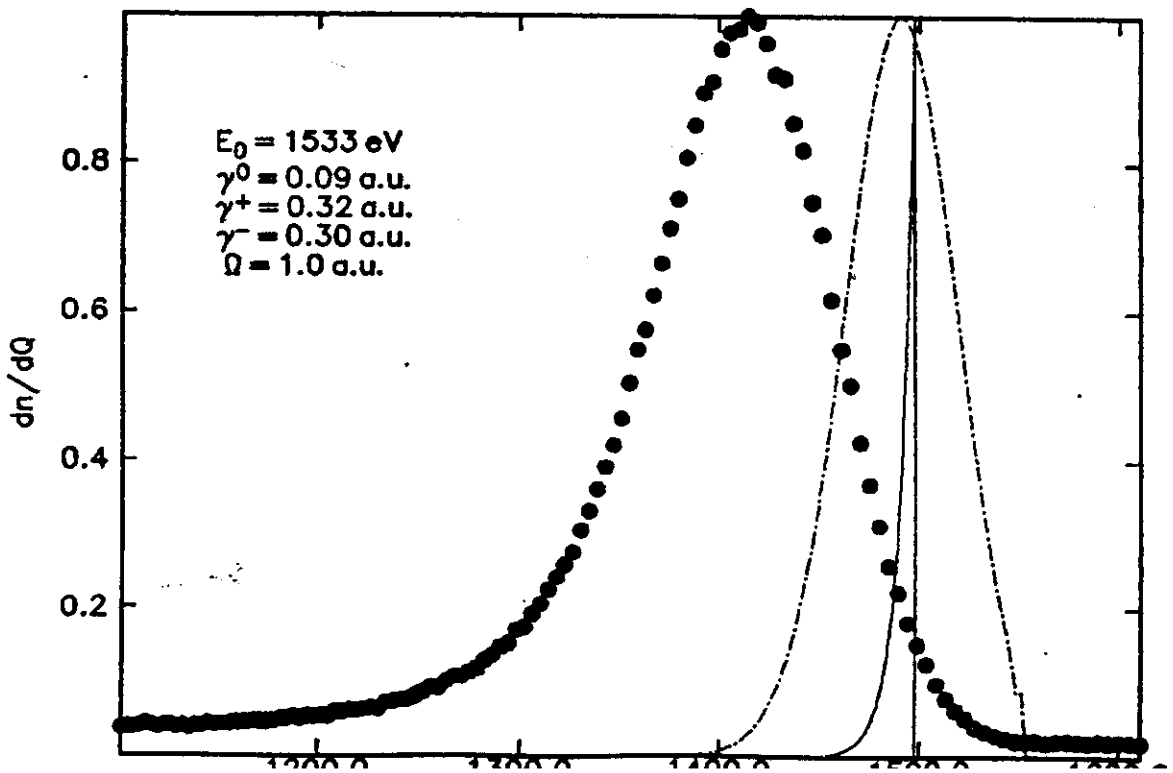

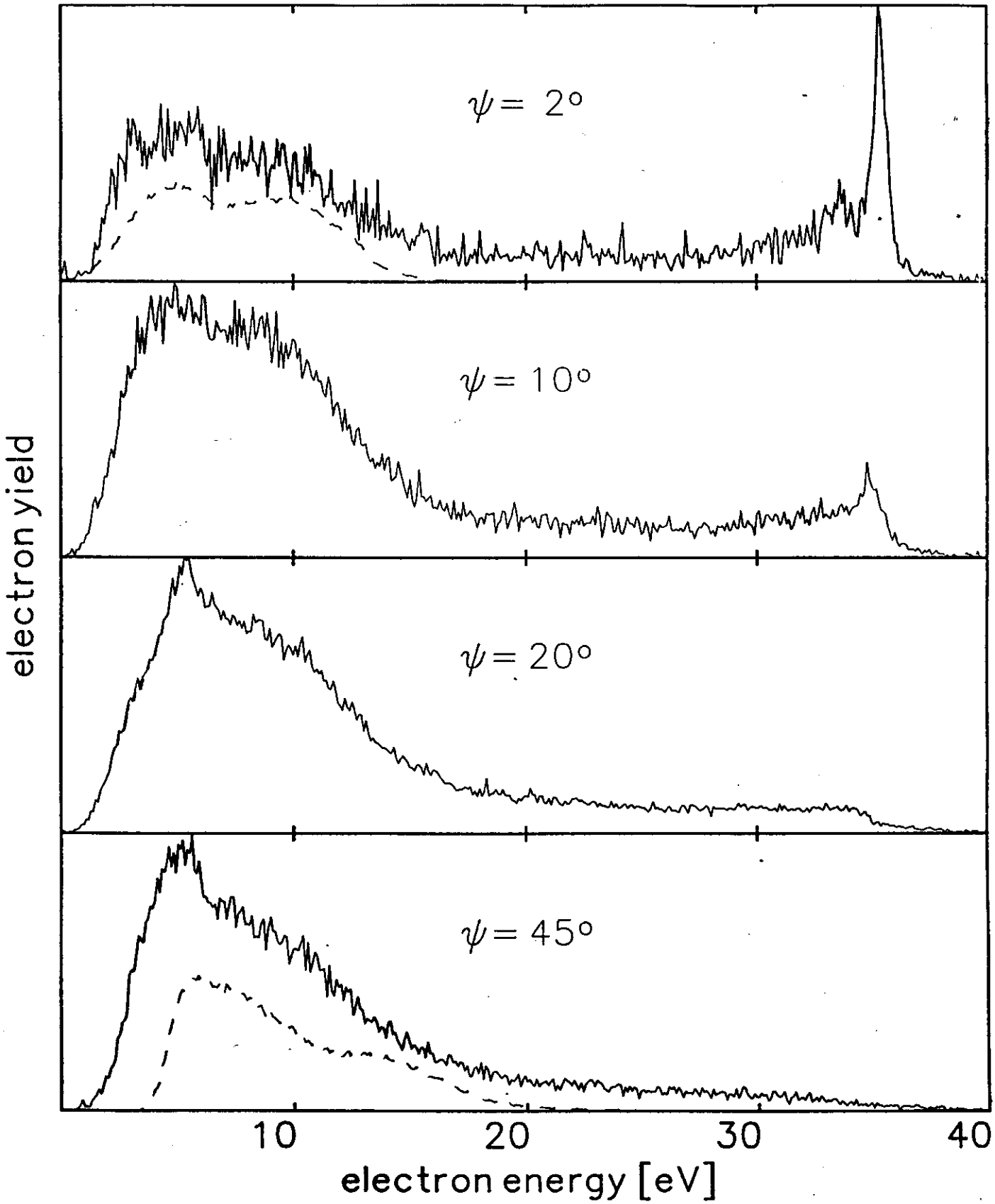

Electron spectra from He^{++} -> Pb(111) (full lines) and He^{+} -> Pb(111) (broken lines) for different angles of incidence and E_{kin} = 1 keV.
The abcissae of the He^{+} curves are not to scale.

S. Schippers et al Surf Sci '92

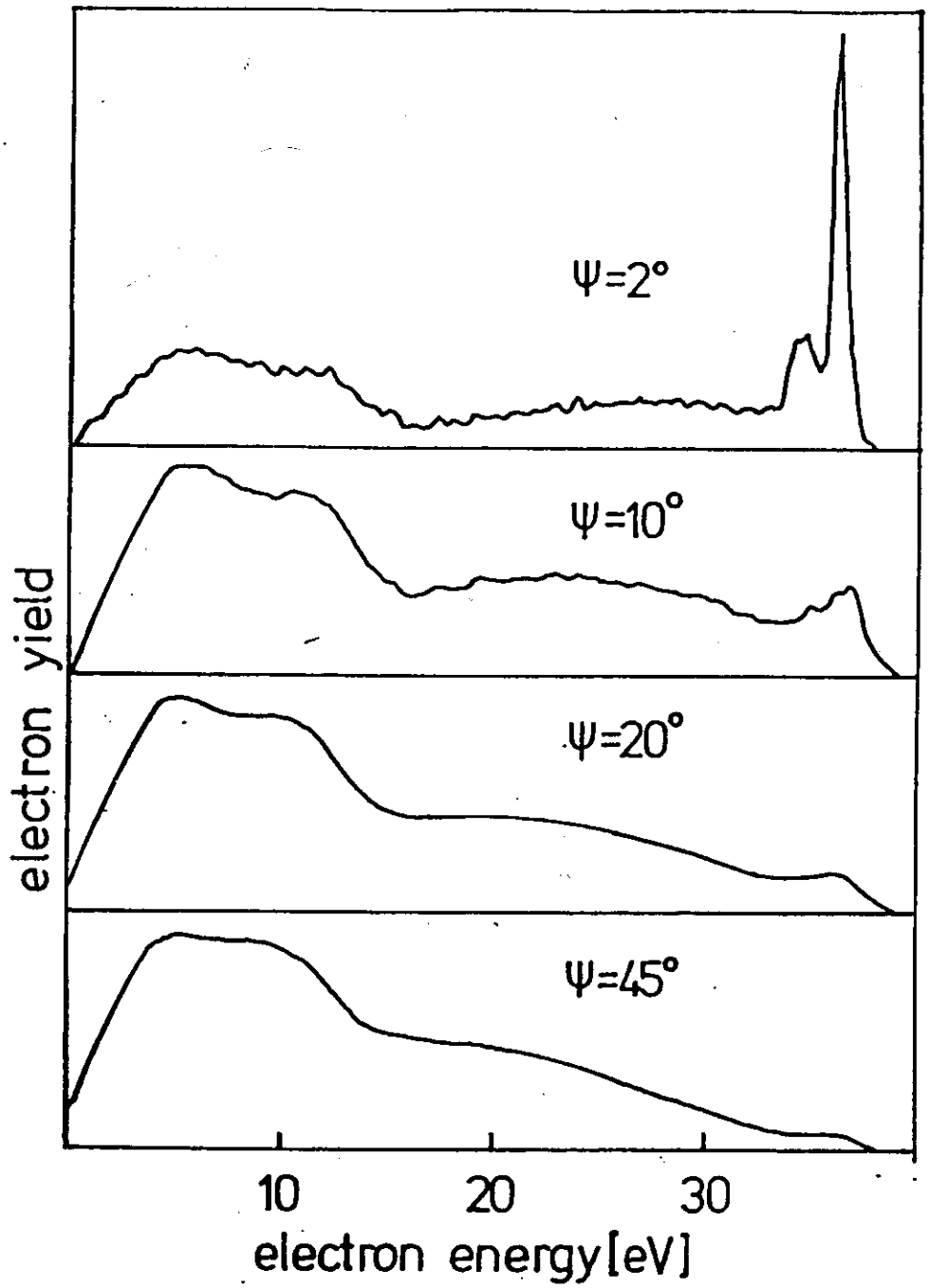

Calculated electron spectra for $He^{++} \rightarrow Pb(111)$, E_{kin} = 1keV, impact angle as parameter.

The following table lists the relevant spectral contributions together with the maximum values of the respective transition rates:

AC(1,0)	$3.0 \times 10^{15} s^{-1}$
AC(2,0)	$1.7 \times 10^{15} s^{-1}$
RC(2,1)	$9.6 \times 10^{14} s^{-1}$
RC(2,0)	$4.2 \times 10^{14} s^{-1}$
AU(2,2) - $He^{**}(2s^2)^1S$	$1.7 \times 10^{14} s^{-1}$ §
AU(2,2) - $He^{**}(2p^2)^1D$	$8.3 \times 10^{13} s^{-1}$ §

Tully
Heiland
PRL
1978

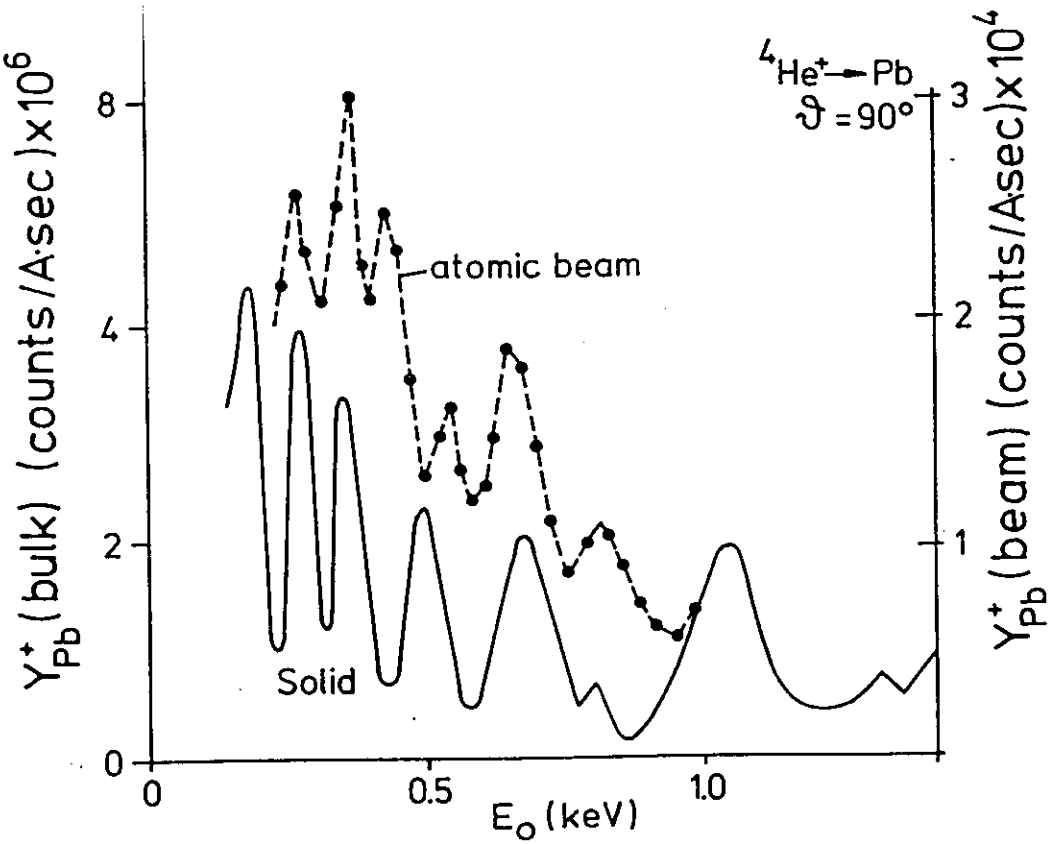

J. Tully
PRB
1977

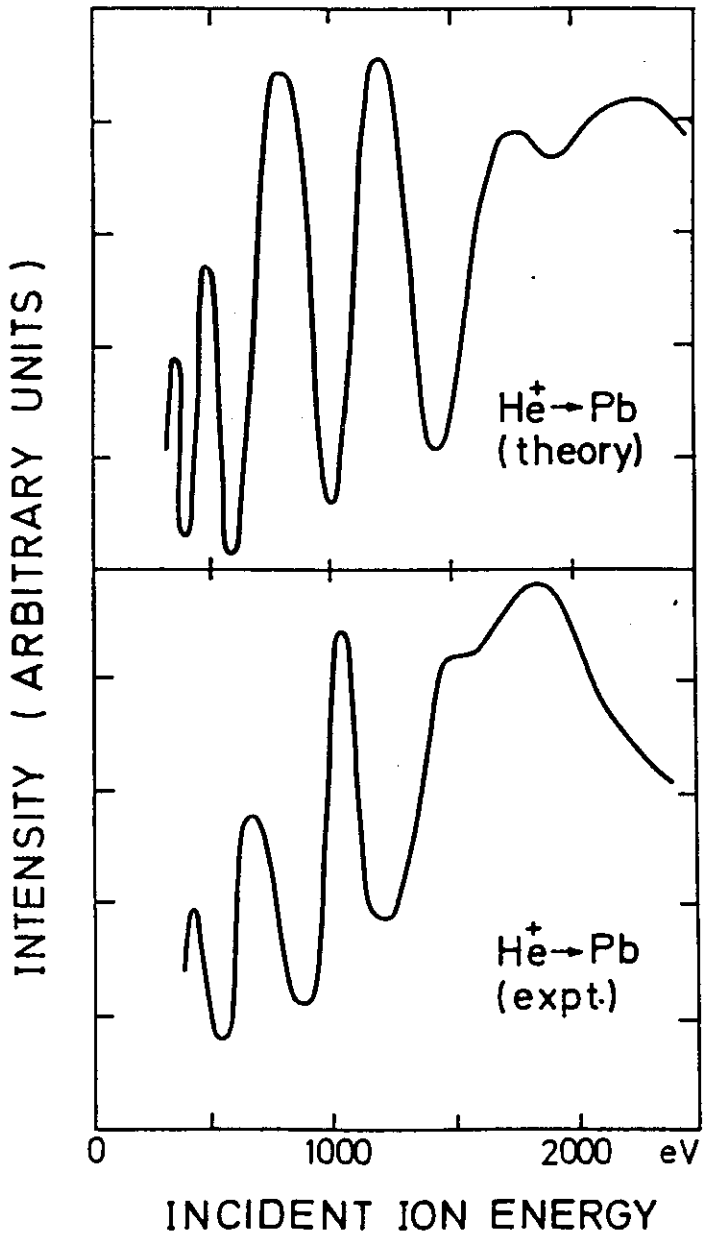

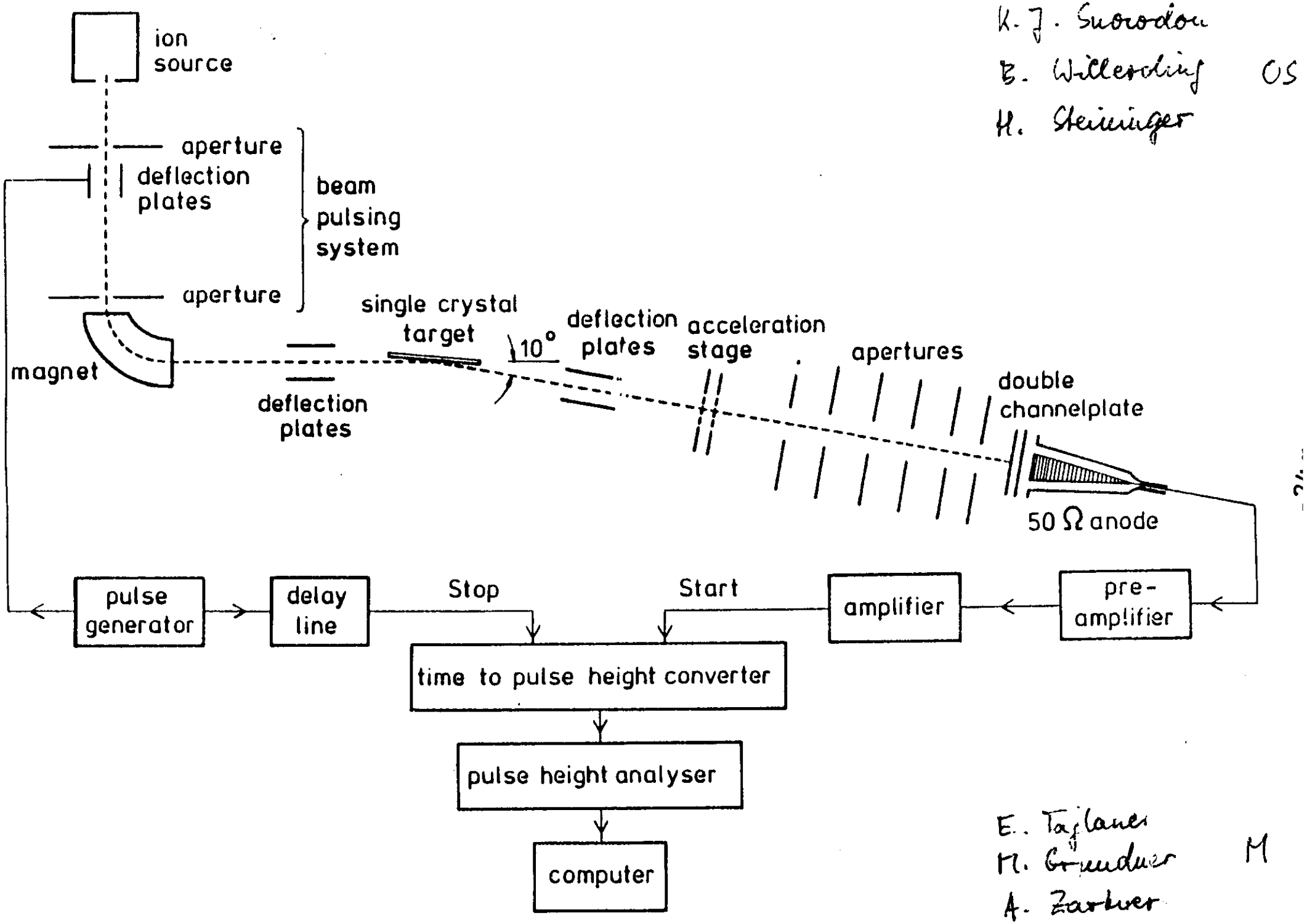

K. J. Snowdon
B. Willerding OS
H. Steininger

E. Taglauer
M. Grundner M
A. Zartner

Eckstein, Verbeek and Dahl 1975. A.P.L.

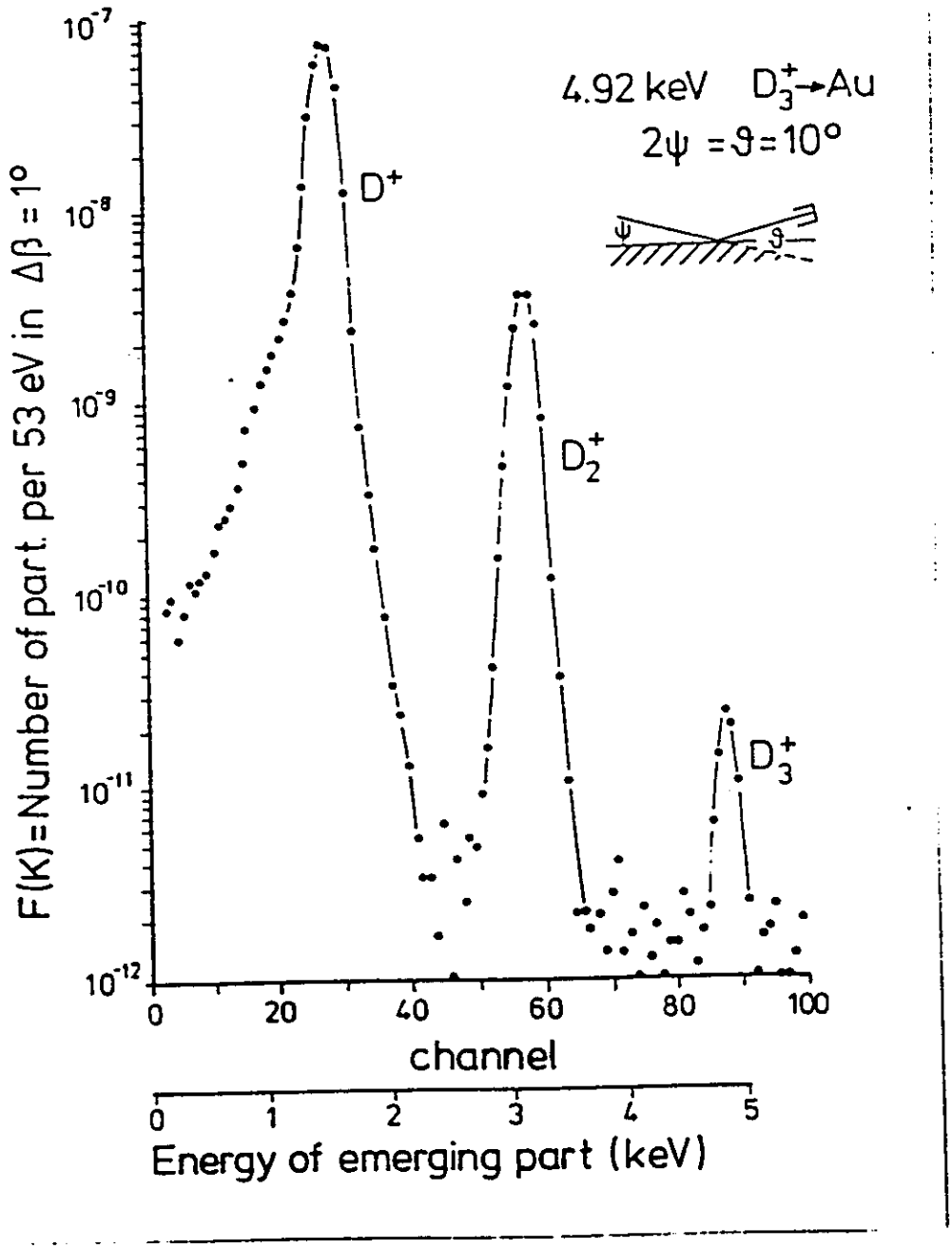

Fig. 29:
Energy spectra of D_3^+ and its dissociation products D_2^+ and D^+ incident at E_o = 4,92 KeV on Au, $\psi = 5°$, $\theta = 10°$. $\Delta\beta$ is the angle of acceptance of the detector (Eckstein et al.[159])

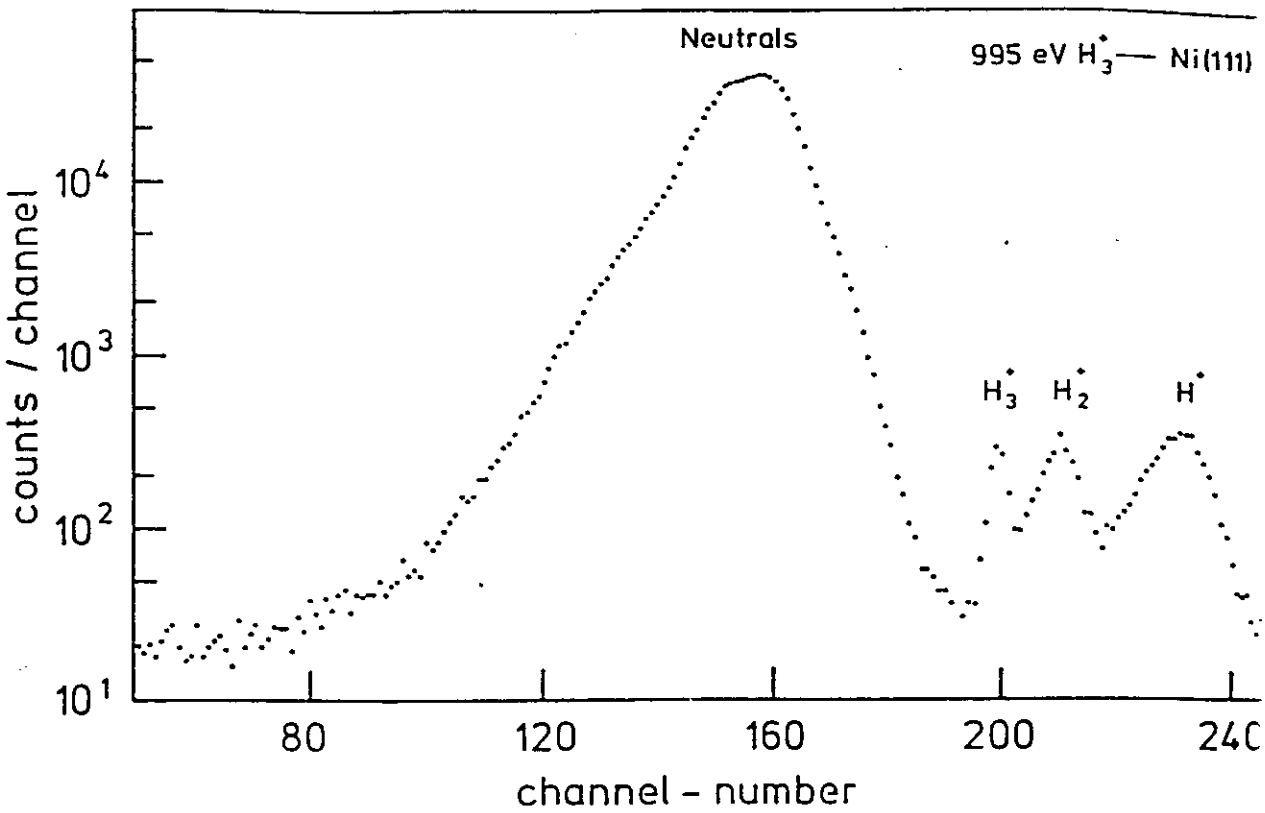

Fig. 30:
Time of flight spectra of H_3^+ and of its ionic and neutral dissociation products, E_o = 495 eV, $\psi = 5°$, $\theta = 10°$ (Willerding et al.[160])

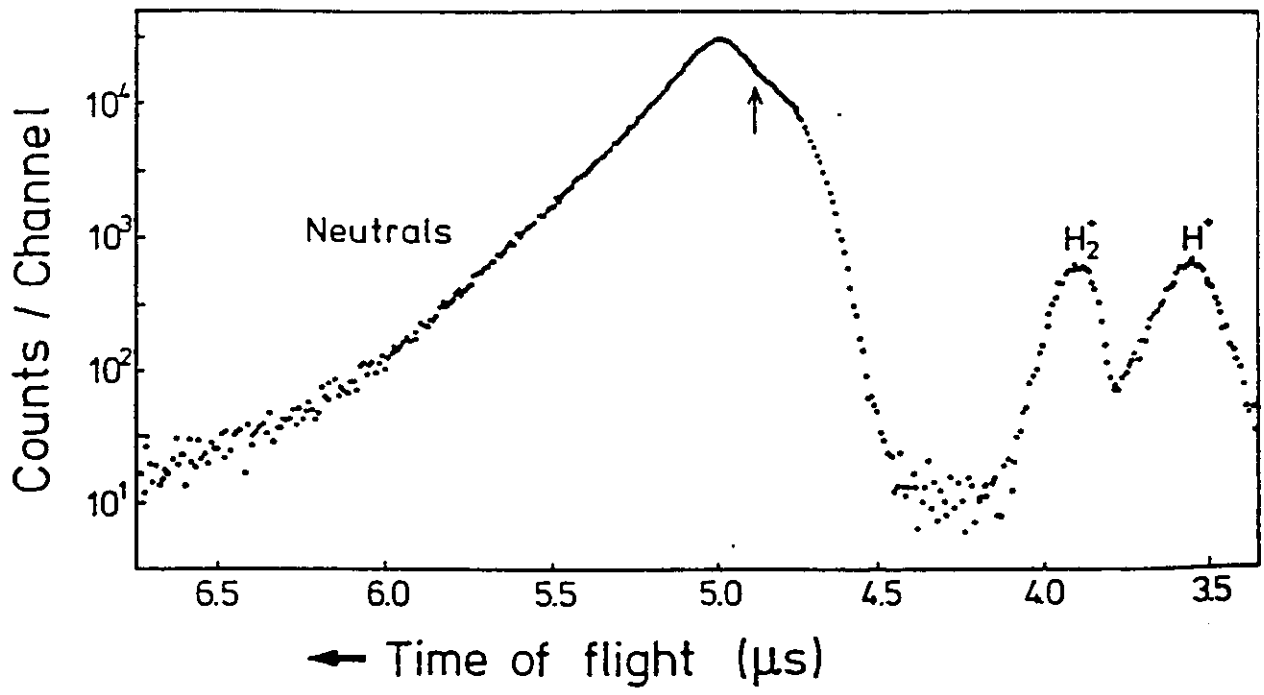

Fig. 31:
Time of flight spectra of H_2^+ and of its dissociation products from Al(111) for E_o = 200 eV (Imke[161])

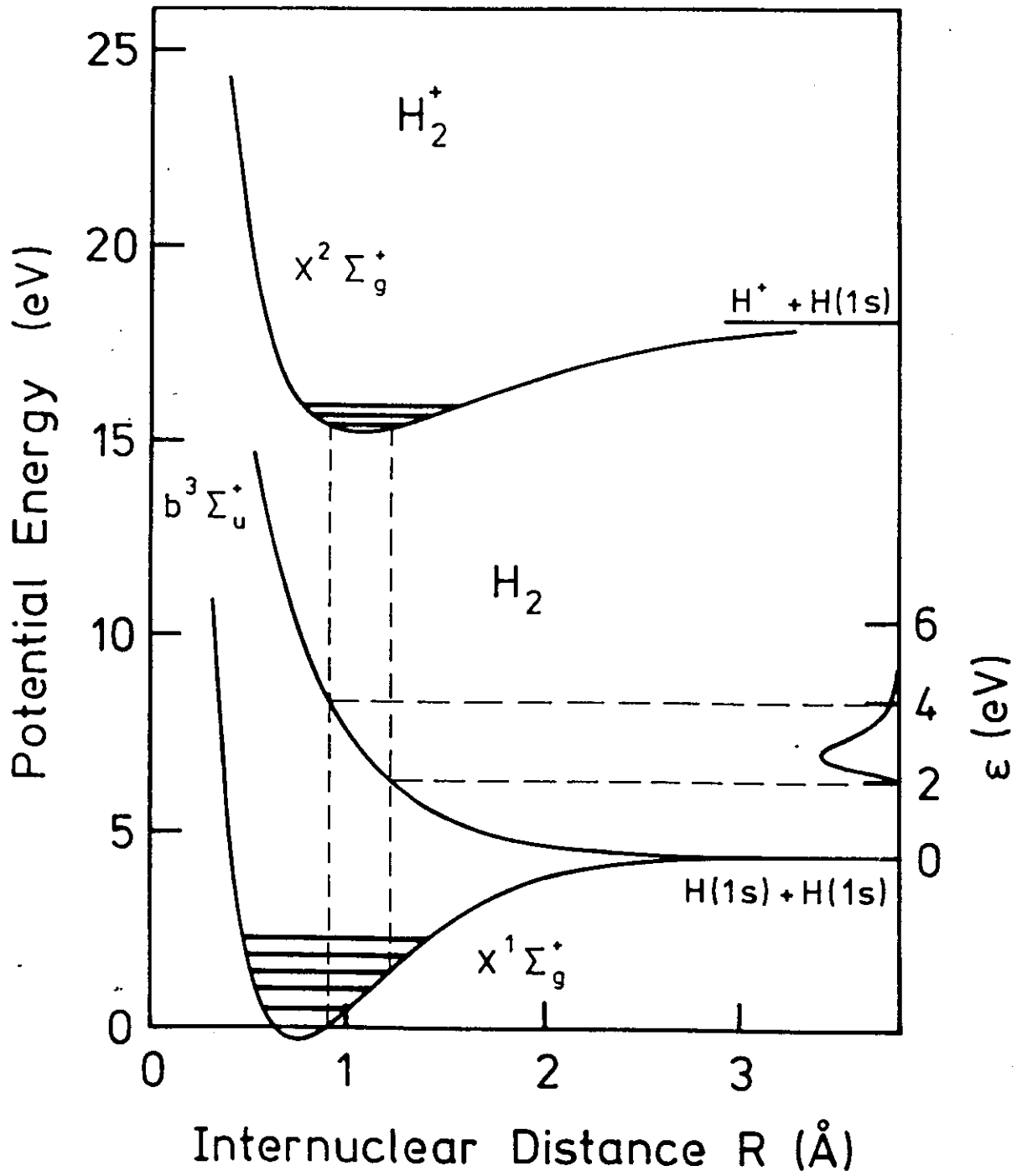
25
20
15
10
5
0
Potential Energy (eV)
H_2^+
$X^2\Sigma_g^+$
$H^+ + H(1s)$
$b^3\Sigma_u^+$
H_2
$x^1\Sigma_g^+$
$H(1s) + H(1s)$
6
4
2
0
ε (eV)
0
1
2
3
Internuclear Distance R (Å)

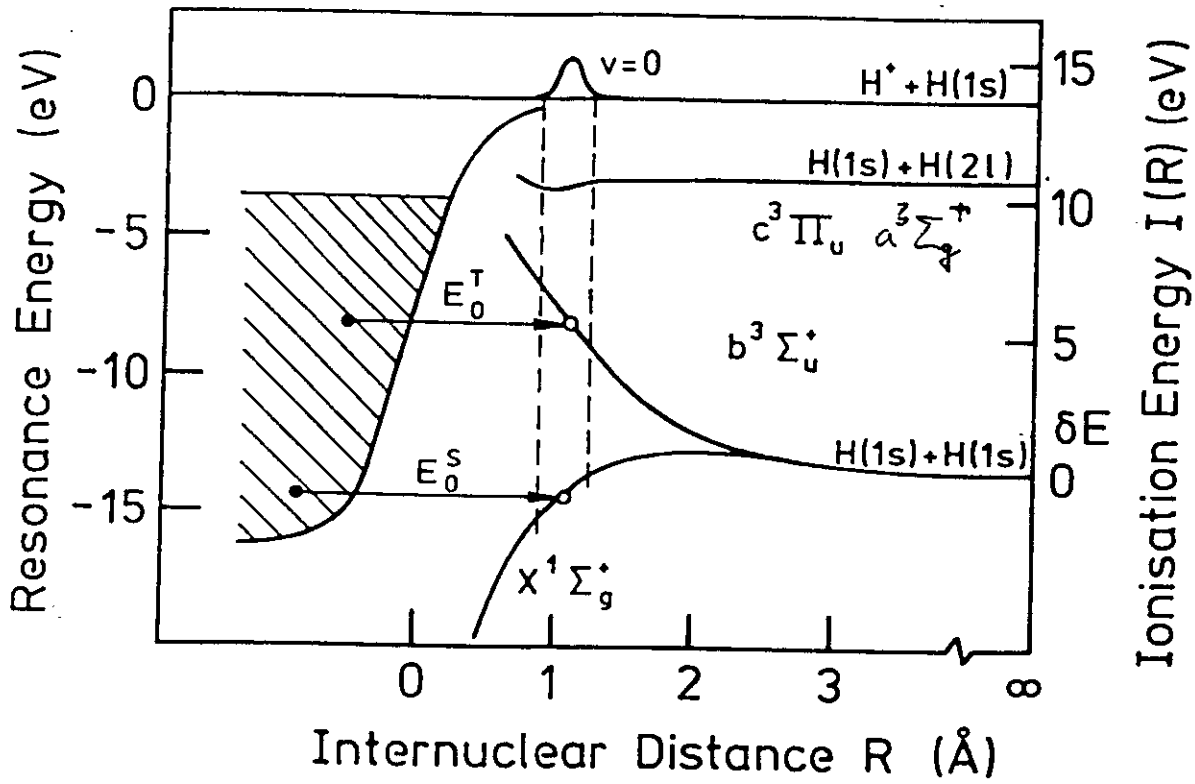
Resonance Energy (eV)
0
-5
-10
-15
v=0
H⁺+H(1s)
H(1s)+H(2l)
c³Πu a³Σg⁺
b³Σu⁺
H(1s)+H(1s)
X¹Σg⁺
E₀ᵀ
E₀ˢ
15
10
5
δE
0
Ionisation Energy I(R) (eV)
0
1
2
3
∞
Internuclear Distance R (Å)

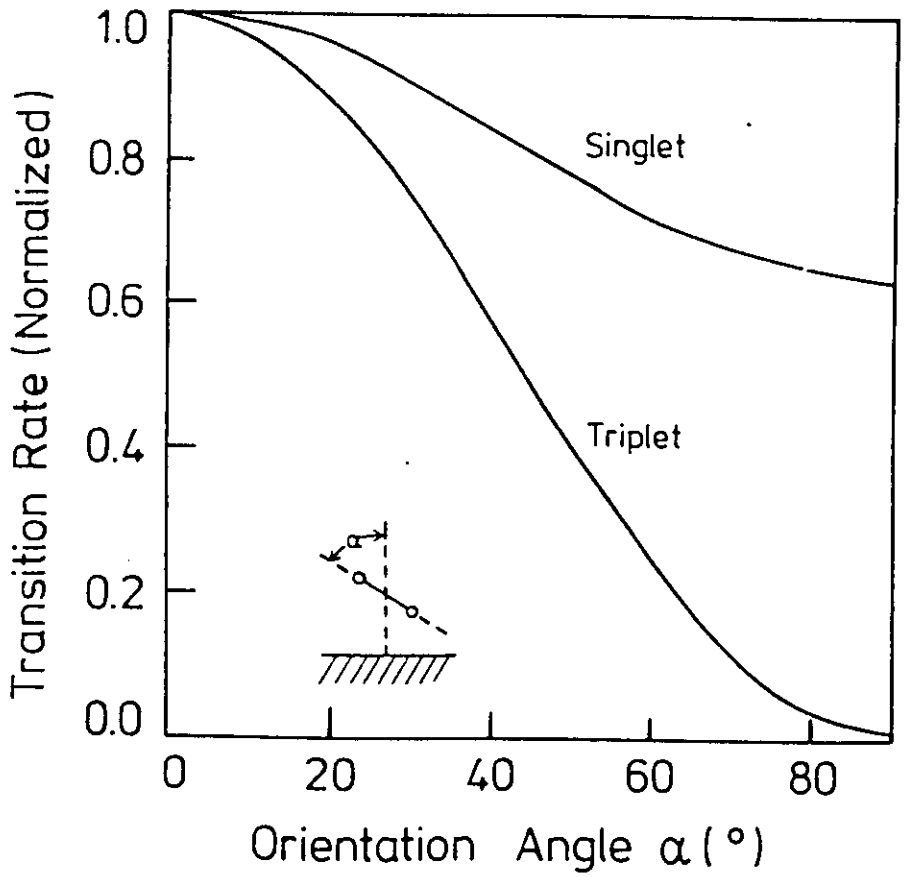
Transition Rate (Normalized)
1.0
0.8
0.6
0.4
0.2
0.0
Singlet
Triplet
α
0
20
40
60
80
Orientation Angle α(°)

Transition probabilities and Symmetry considerations (G. H. Dunn)

Initial state	orientation	final state $N_2, H_2, N+N, \Sigma_g^+$	$H+H, O+O\,\Sigma_u^+$	$O+O\,\Pi_g$
H_2^+, N_2^+ Σ_g^+	$\parallel$	Large	Small	
	$\perp$	Large	Large	
$O_2^+\,\Pi_g$	$\parallel$	Small	Large	Large
	$\perp$	Small	Small	Large

U. Imke et al

Al ('jellium') and H_2^+ resonant transitions

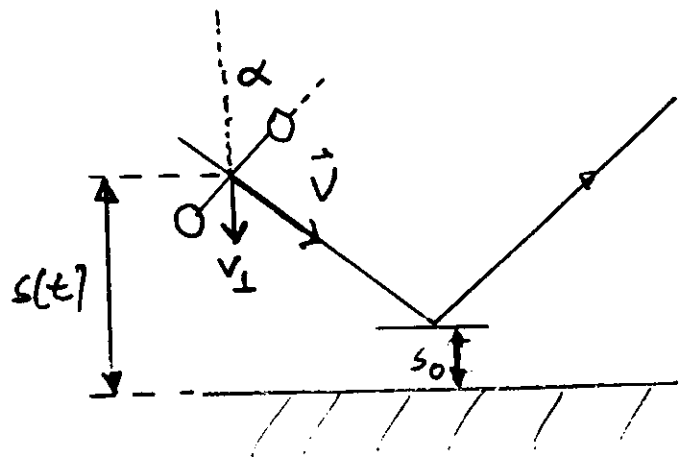

Varga, Schubert, Imke : O_2^+ vs N_2^+

W. Tappe '91
Europhys. Lett

$E_0 = 3keV$; H_2^+

$\psi = 5°$

Ni(110)
⟨random⟩

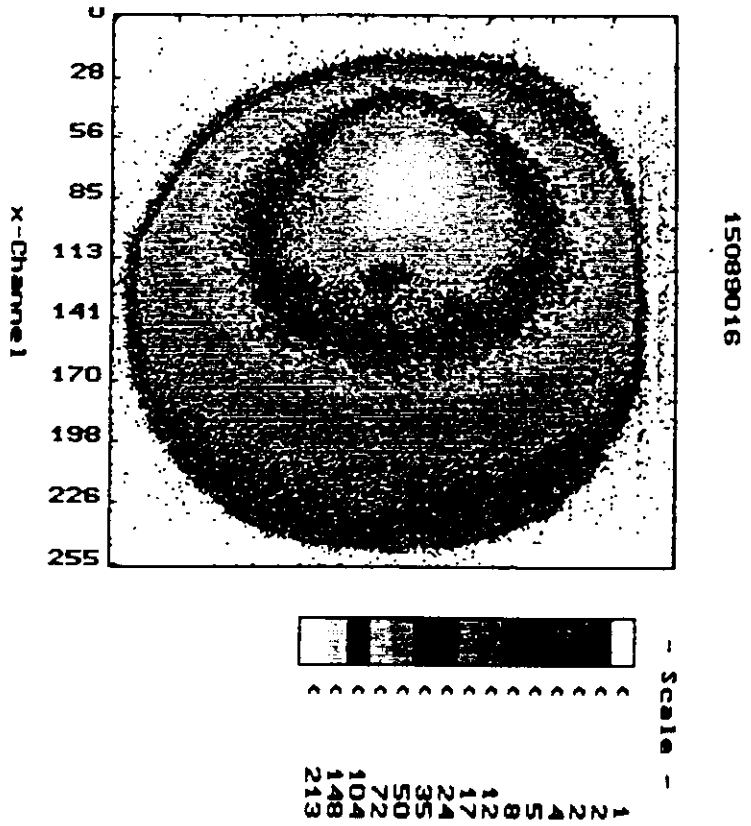

$E_0 = 1.5keV$; H^+

$\psi = 5°$

Ni(110)
⟨random⟩

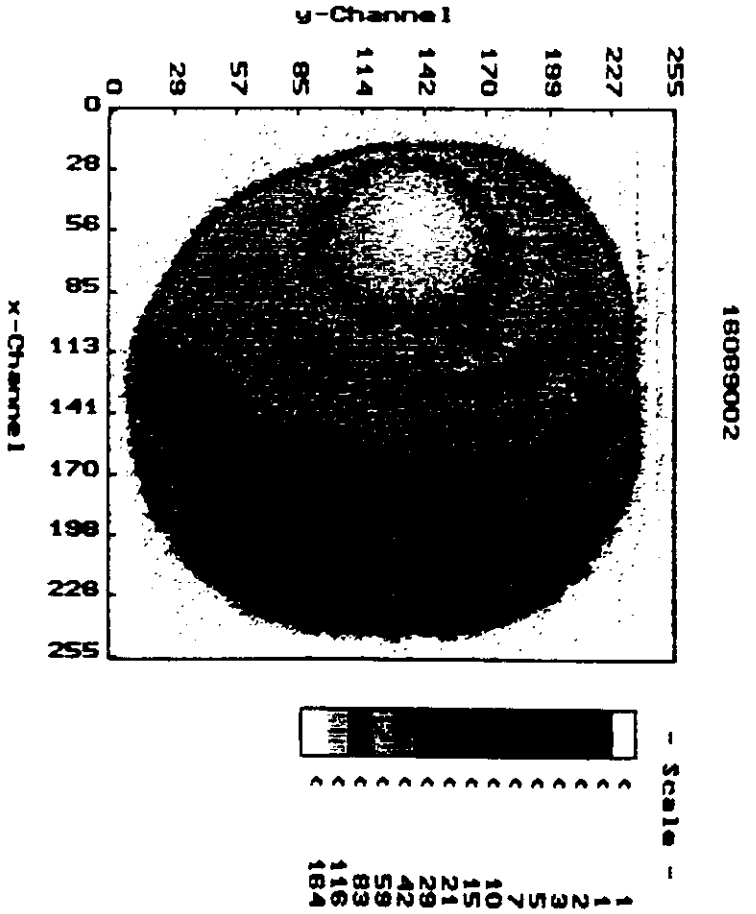

VI Schnitte durch die Streuverteilungen (jeweils durch das Maximum). Die Schnitte sind normiert.

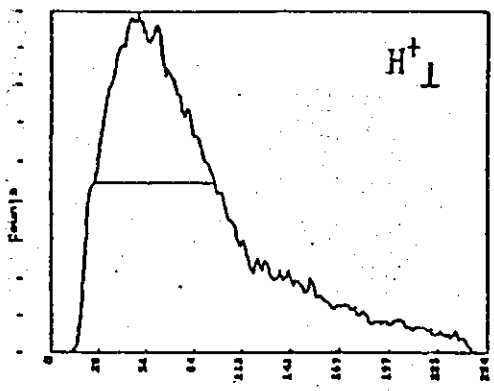

FWHM: 71 Kanäle

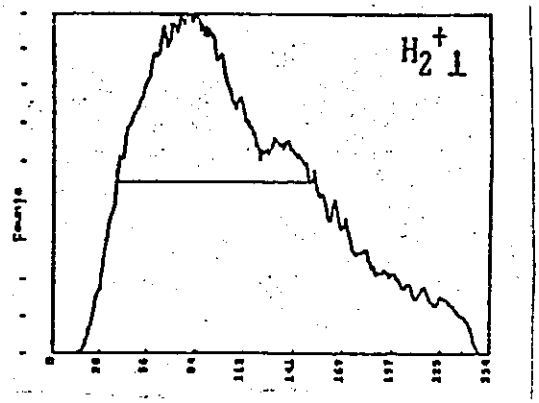

FWHM: 112 Kanäle

$\Delta K = 41$ Kanäle

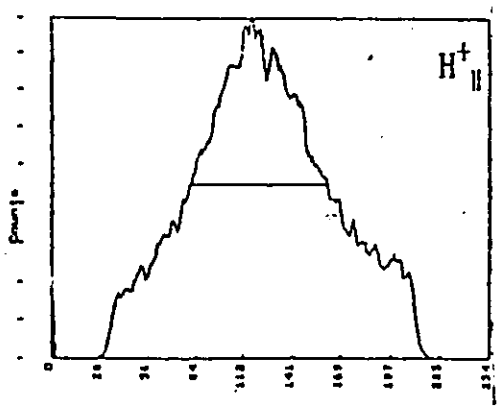

FWHM: 81 Kanäle

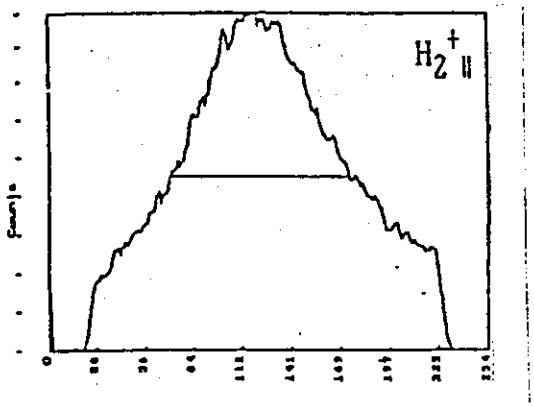

FWHM: 103 Kanäle

$\Delta K = 22$ Kanäle

Ergebnis:
- Aufweitung des molekularen Strahls gegenüber dem atomaren Strahl
- senkrecht zur Oberfläche ($\perp$) ist diese Aufweitung ($\Delta K = 41$ Kanäle) größer als parallel ($\parallel$) zur Oberfläche ($\Delta K = 22$ Kanäle)

Efficiency and Particle

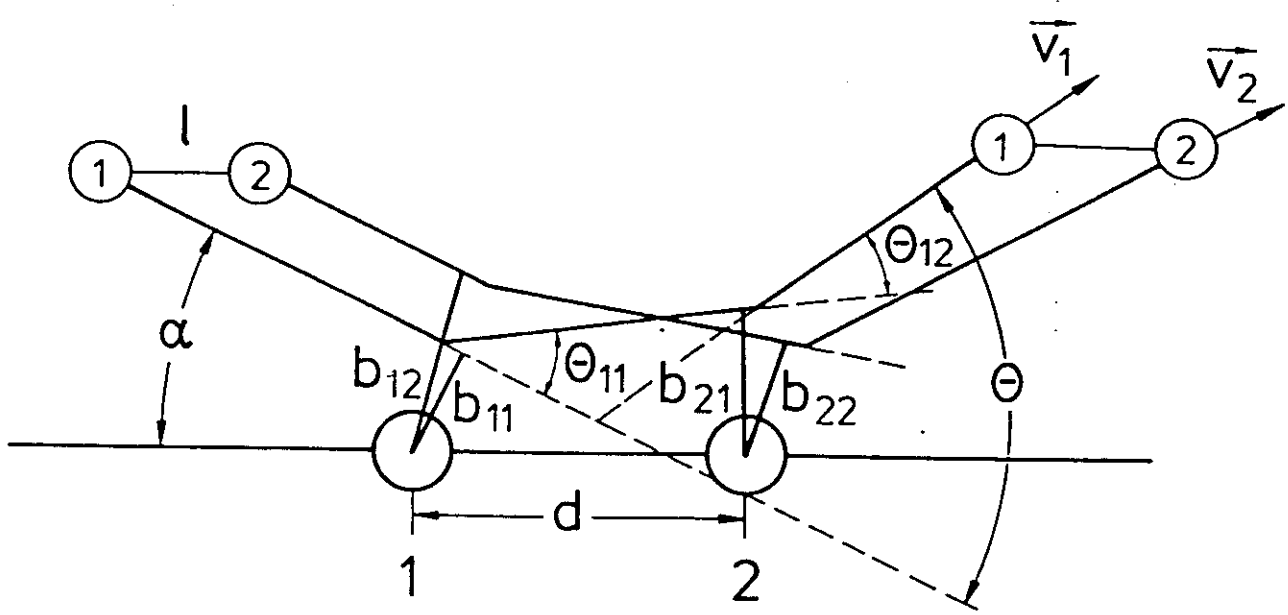

W. N. Sachsen 1986

Oberfläche

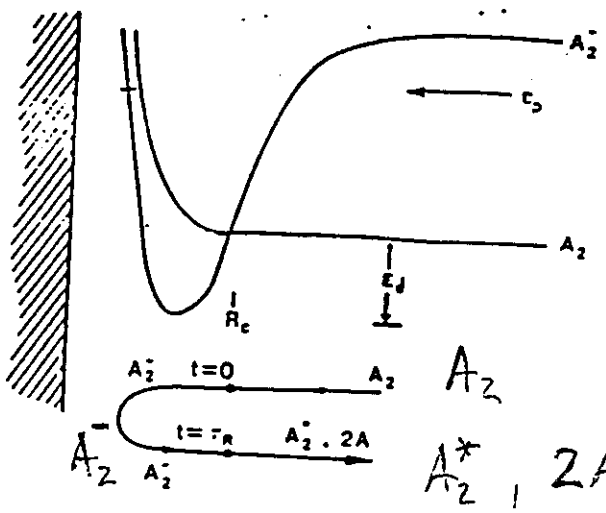

A_2^- ↑ $\Phi - E_a$ ↓ A_2 (a)

A_2 A_2^*, 2A (b)

Vibrational excitation in Molecule - Surface Collisions

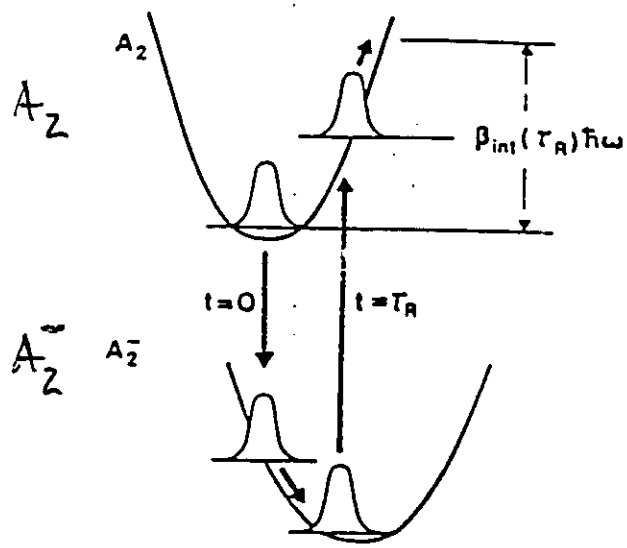

(c)

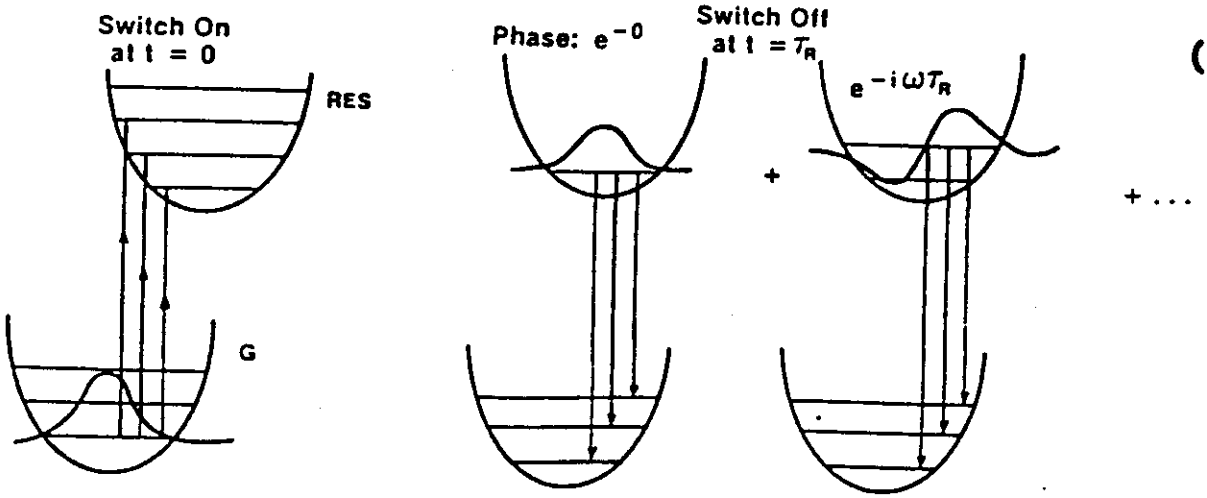

(d)

K. Hashimura, F. Schmidt-Bleek and S. Datz
J. Chem. Phys. 61 (1974) 160

(2)

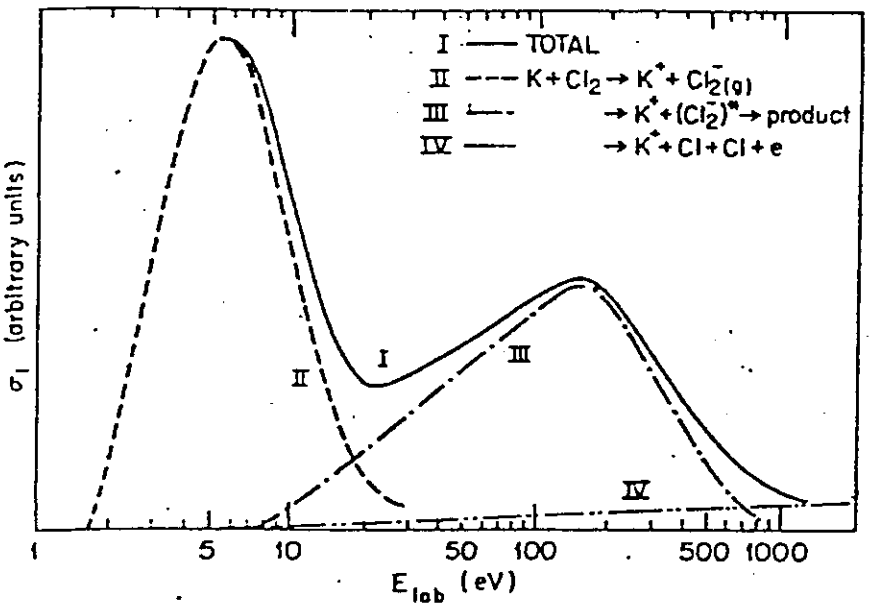

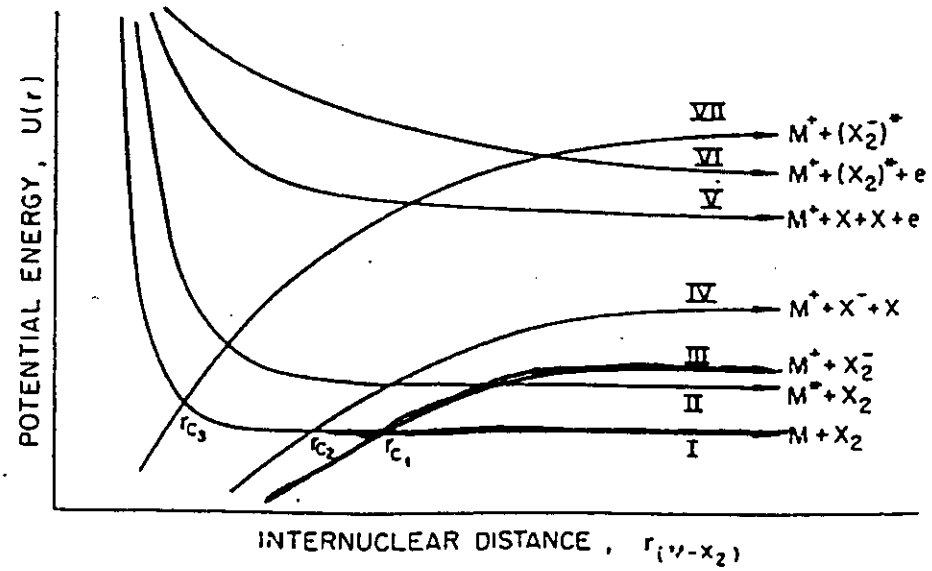

"harpoon model" M. Polanyi
"electron jump mechanism" D.R. Herschbach

$E_{thr} = I(M) - E(X_2)$

$= \frac{e^2}{4\pi\varepsilon_0 r_{c_1}}$

"pseudocrossing of the homopolar and ionic potential energy surface"

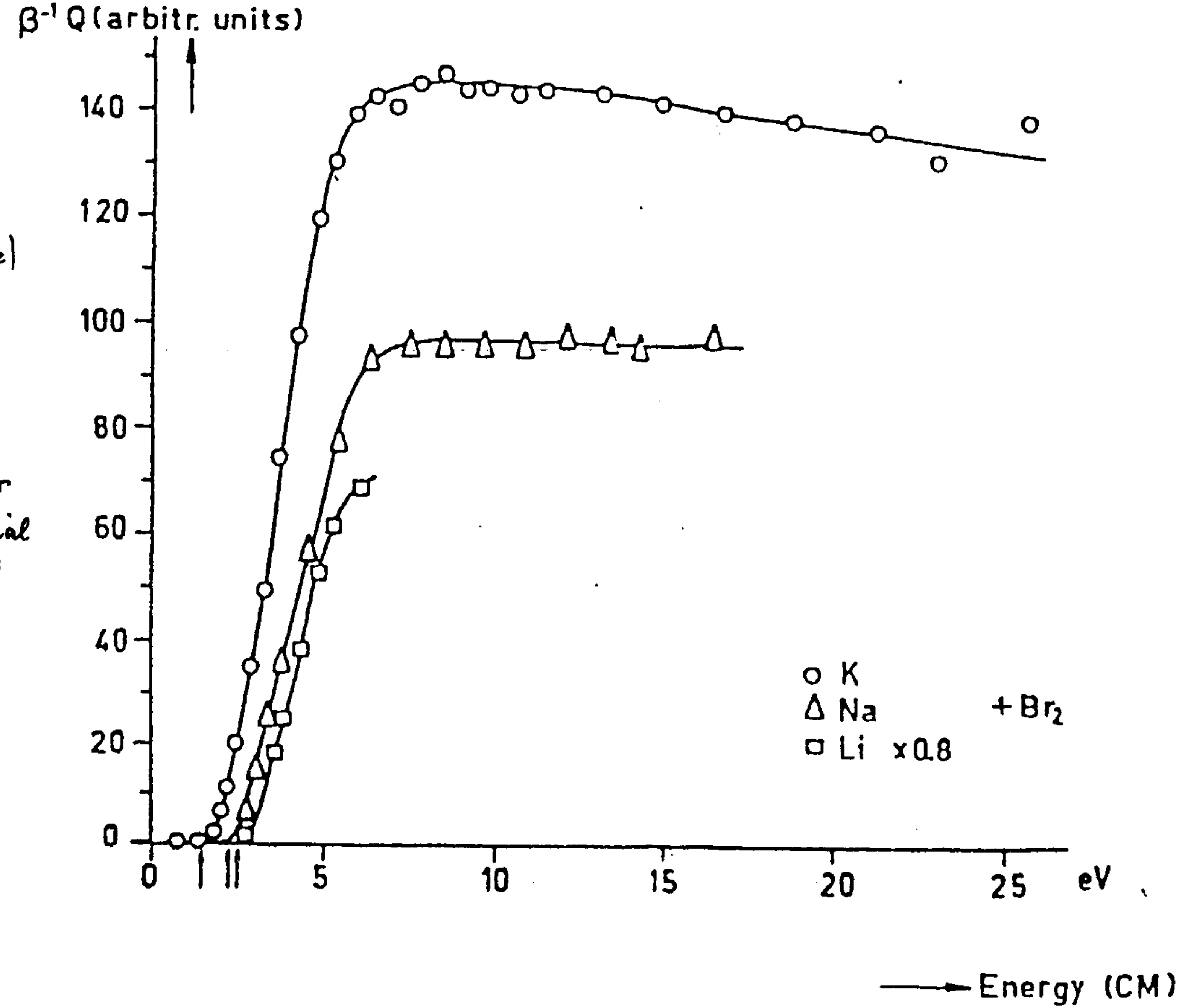

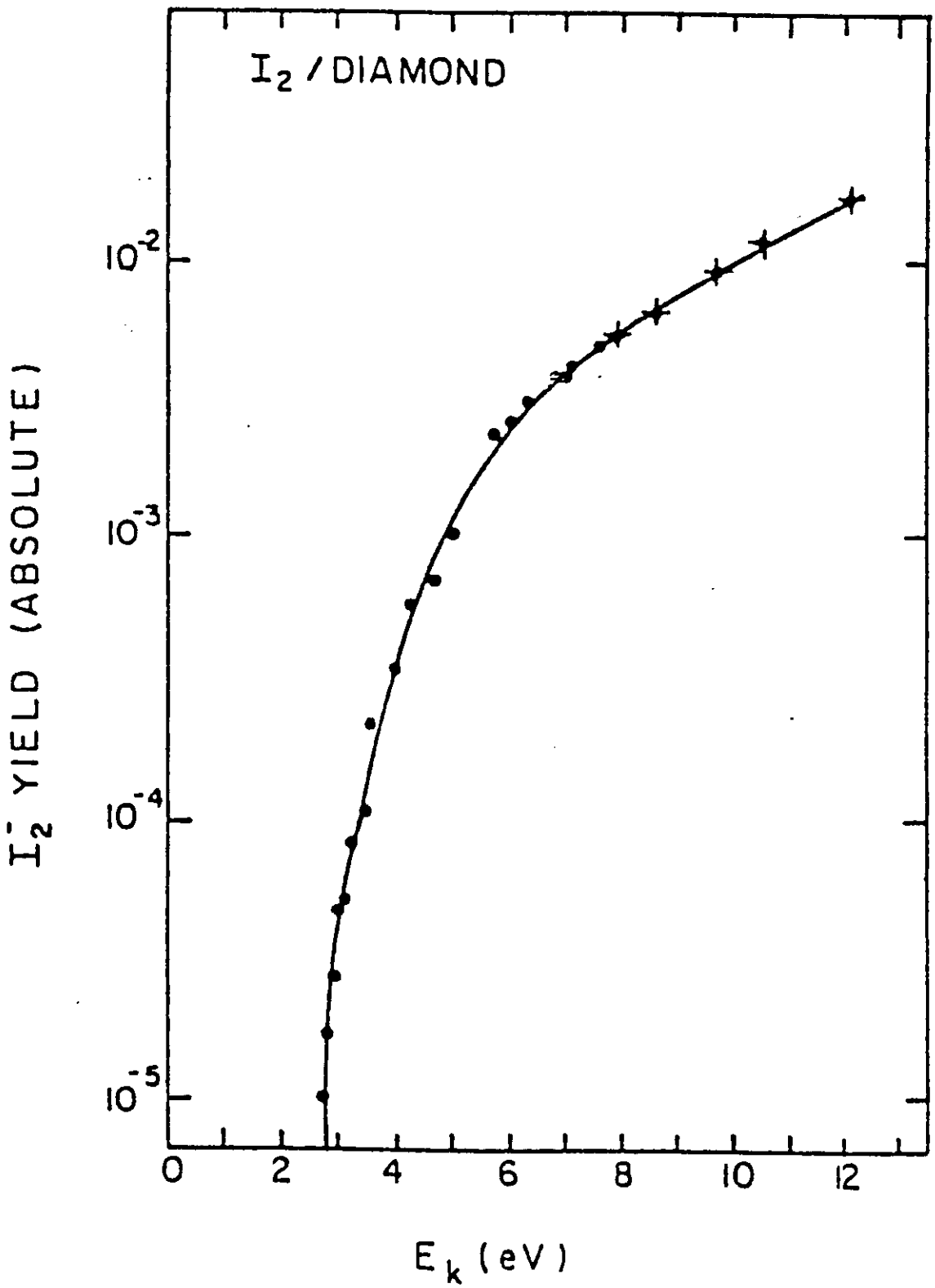
I2 / DIAMOND
I2- YIELD (ABSOLUTE)
10-2
10-3
10-4
10-5
0
2
4
6
8
10
12
Ek (eV)

PHF Reijnen and A.W. Kleyn Chem. Phys. 154 (1991) 23
AW Kleyn Vacuum 41 (1990) 248

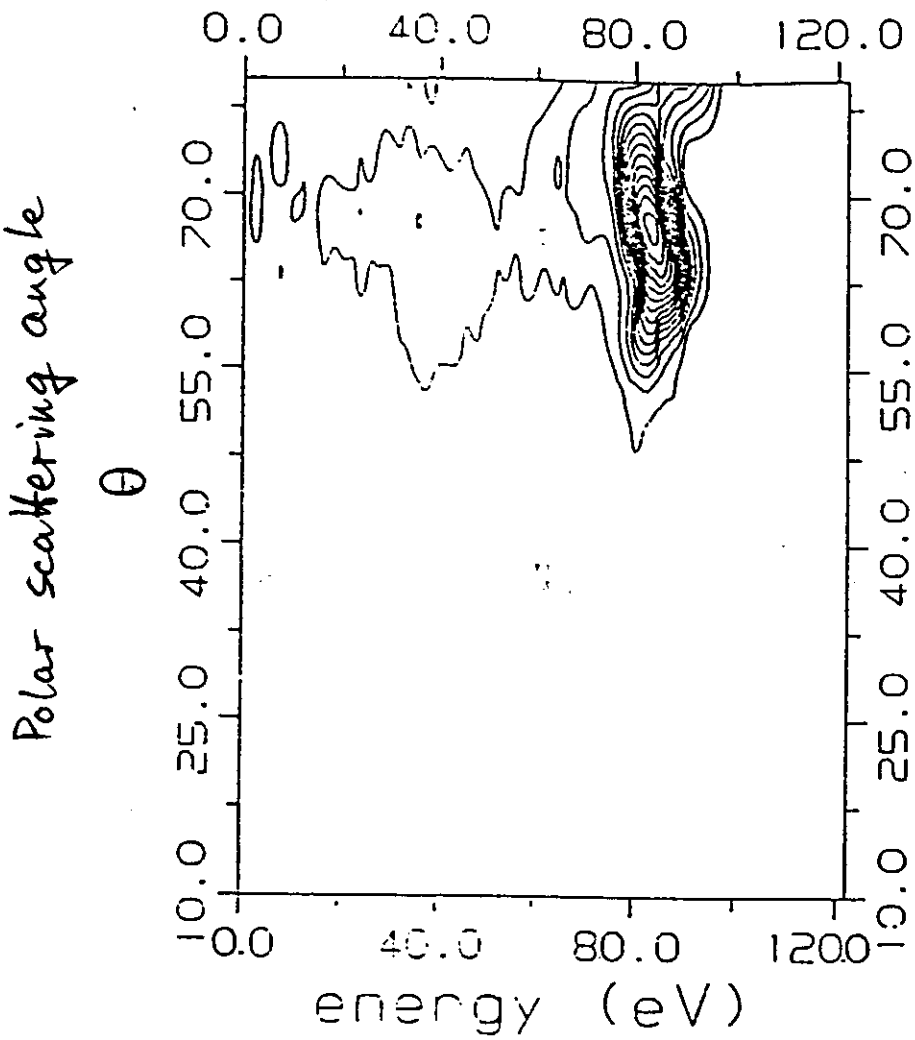

100 eV $O_2 \rightarrow Ag(111)$
$\psi = 20°$

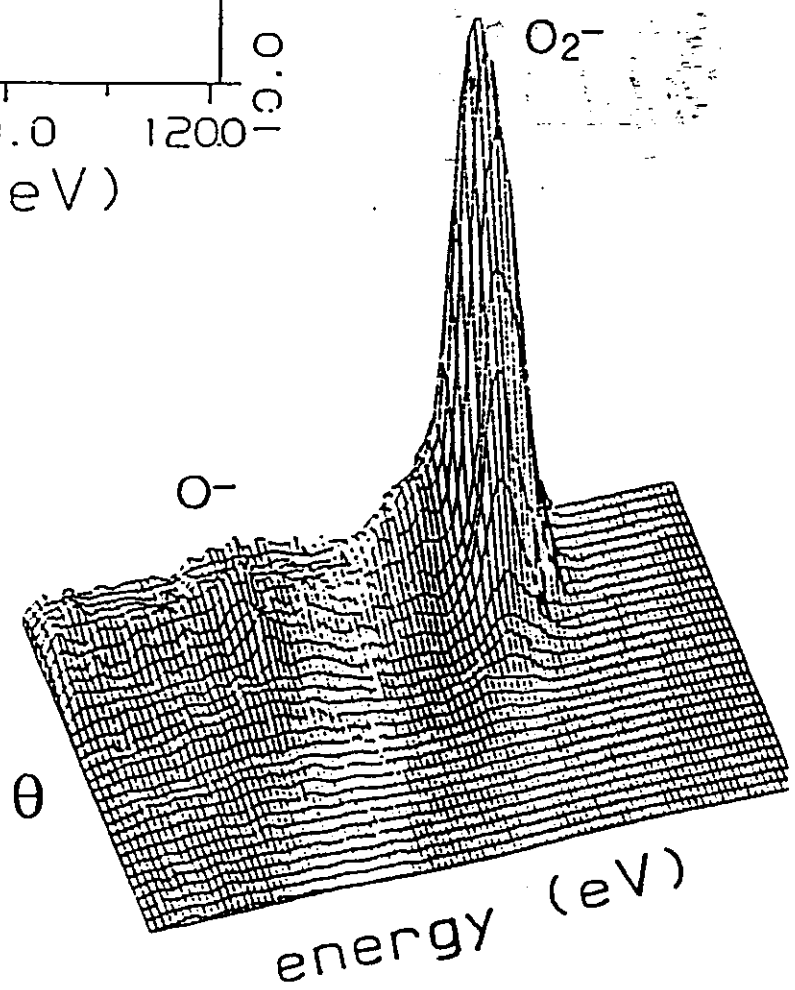

an Haochang
T.C.M. Horn
A.W. Kleyn
R.L. 57
1986) 3035

$O_2^+ \rightarrow O^- + O_2^-$
Ag(111)

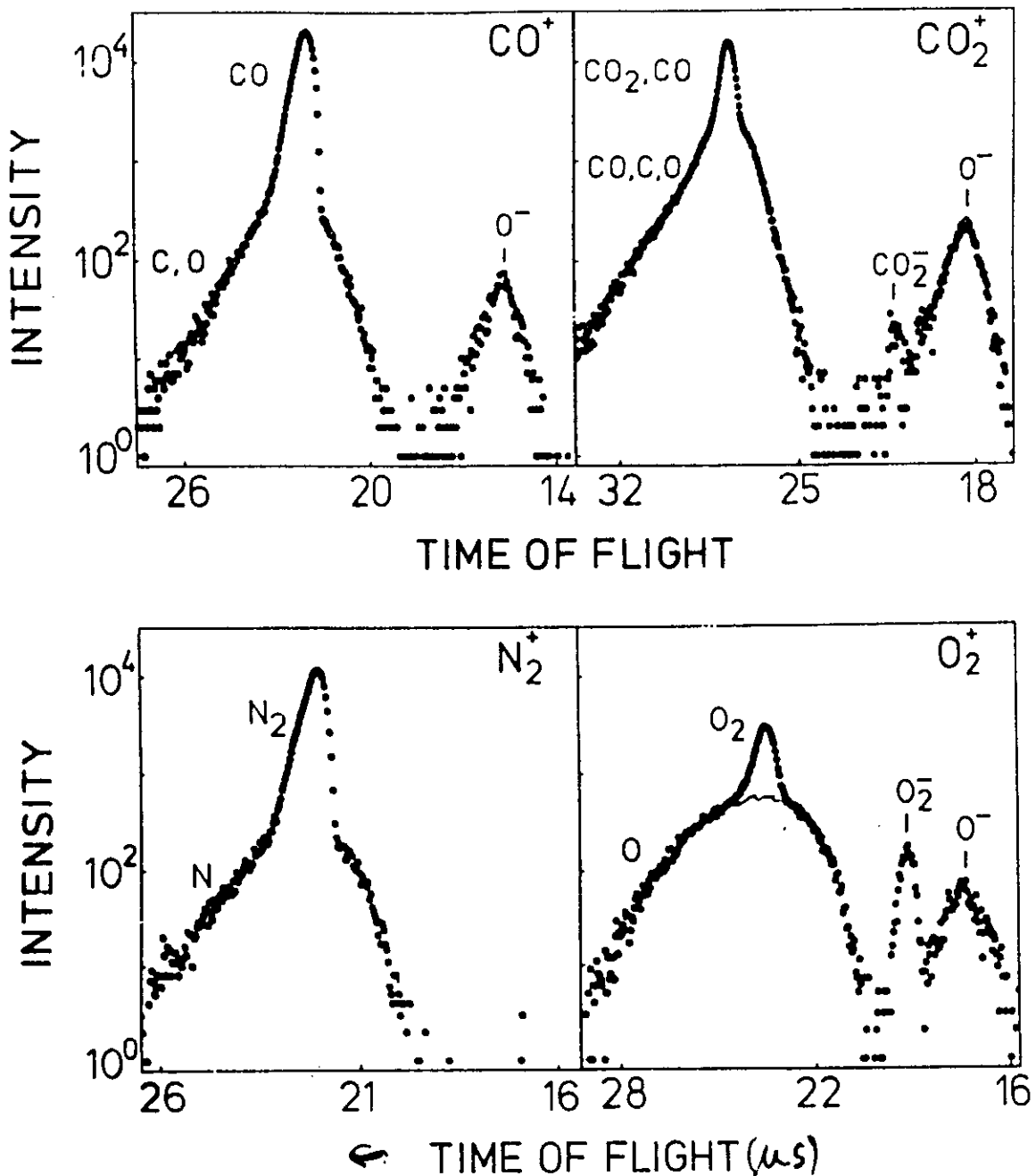

A. Kleyn FOM
P. Reijnen "
S. Schubert OS
U. Imke "
H. Rechtien "

Ni

Pan Haochang et al FOM

Ag

-386-

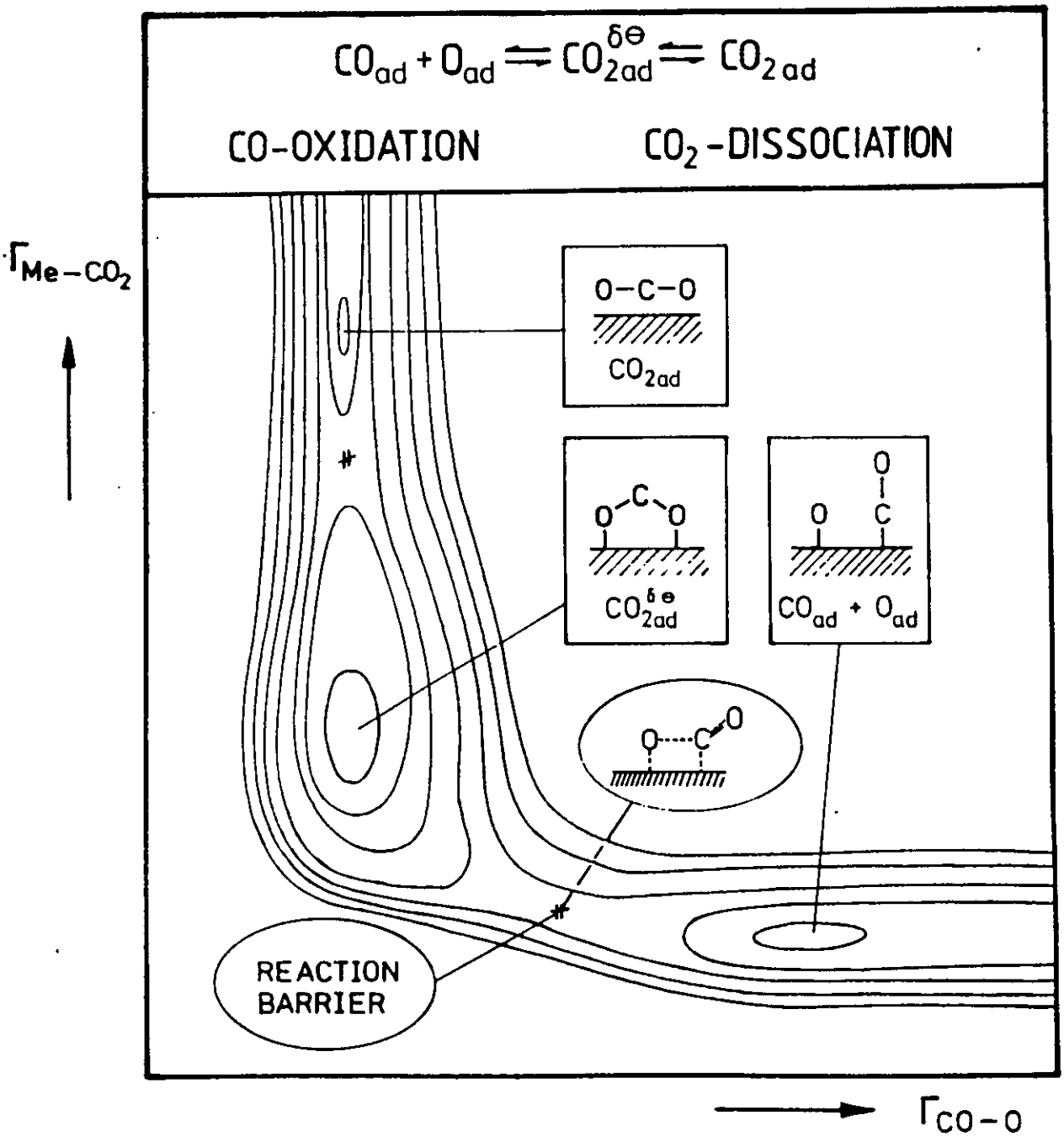
$CO_{ad} + O_{ad} \rightleftharpoons CO_{2ad}^{\delta\Theta} \rightleftharpoons CO_{2\,ad}$
CO-OXIDATION
CO_2-DISSOCIATION
Γ_{Me-CO_2}
O–C–O
CO_{2ad}
$CO_{2ad}^{\delta\Theta}$
$CO_{ad} + O_{ad}$
REACTION BARRIER
Γ_{CO-O}

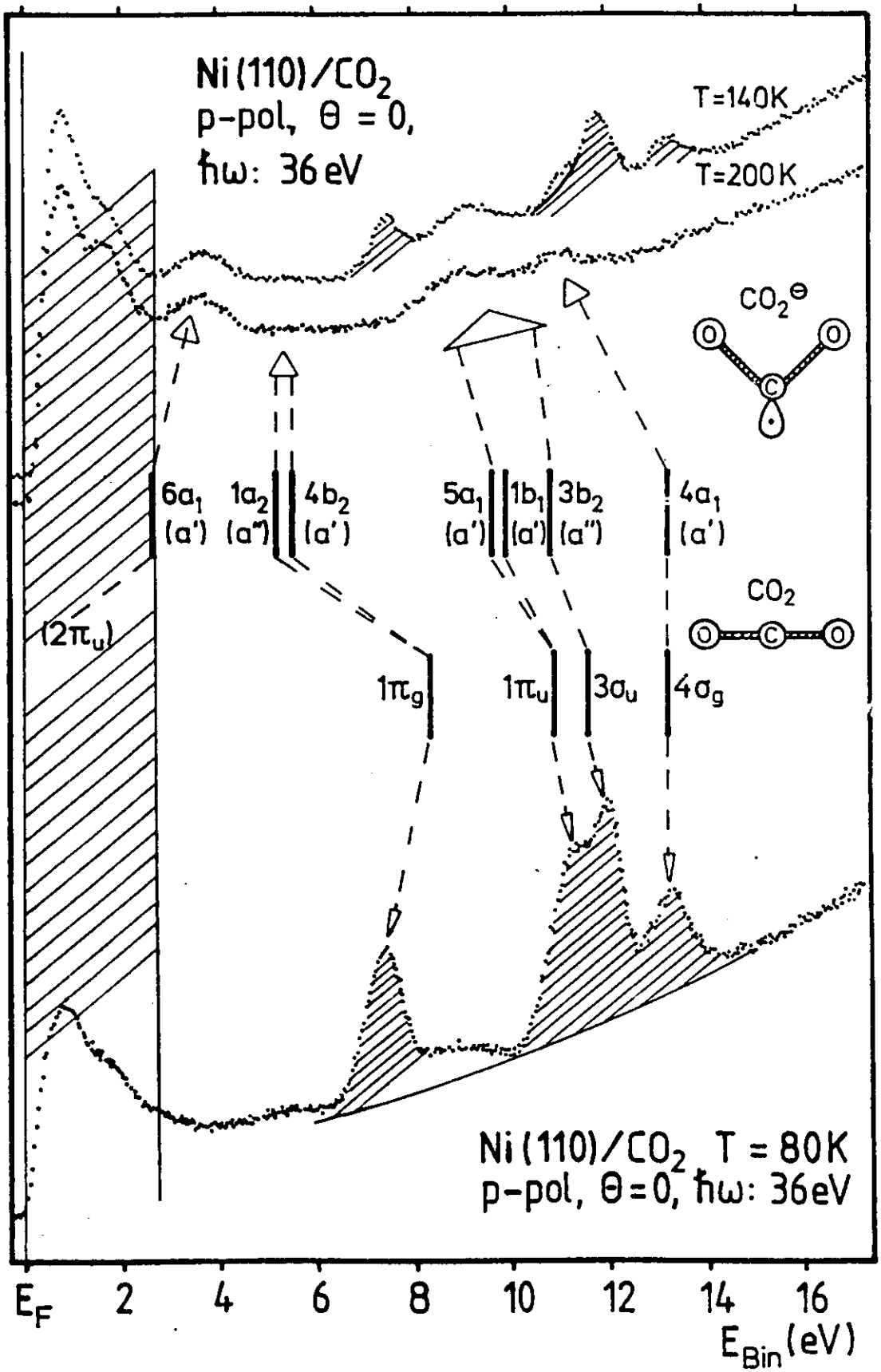
Ni(110)/CO2
p-pol, θ = 0,
ħω: 36 eV
T=140K
T=200K
CO2⊖
6a1 (a')
1a2 (a")
4b2 (a')
5a1 (a')
1b1 (a')
3b2 (a")
4a1 (a')
CO2
(2πu)
1πg
1πu
3σu
4σg
Ni(110)/CO2 T = 80K
p-pol, θ=0, ħω: 36eV
EF
2
4
6
8
10
12
14
16
EBin(eV)

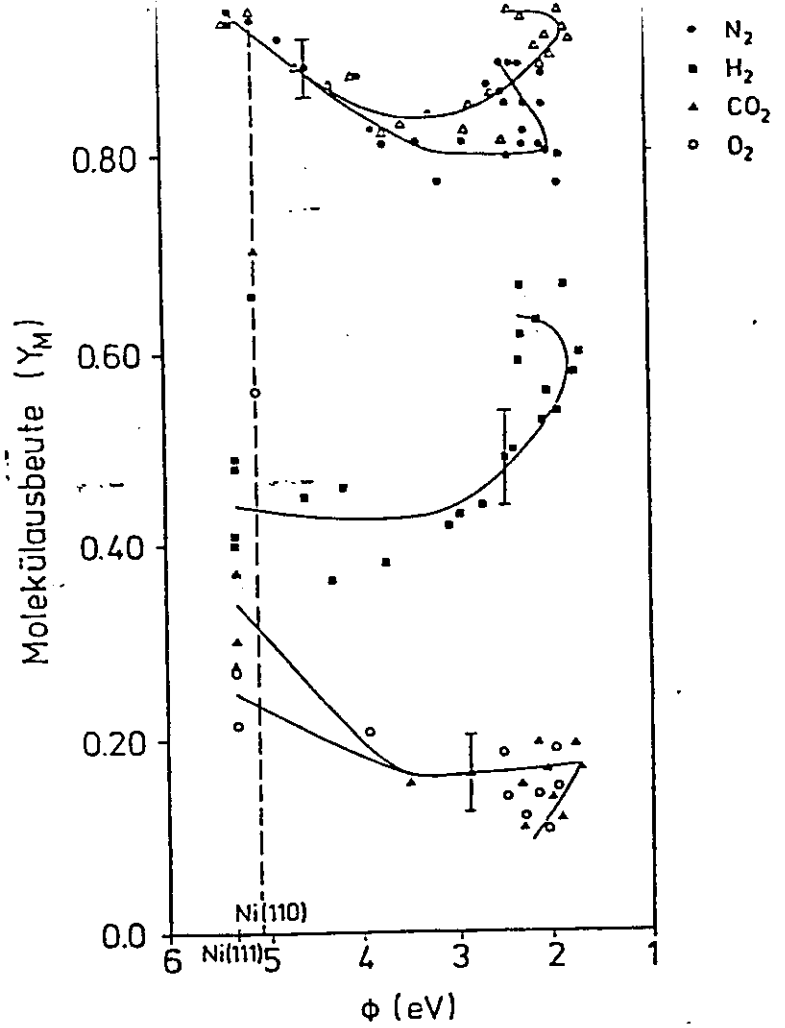

Abb. 20: Die Überlebenswahrscheinlichkeit der unterschiedlichen Molekülarten (Y_M) als Fuktion der Austrittsarbeit (ϕ) der kaliumbedeckten Ni(111)-Oberfläche. Zum Vergleich sind auch die an der Ni(110)-Oberfläche erhaltenen Werte eingezeichnet.

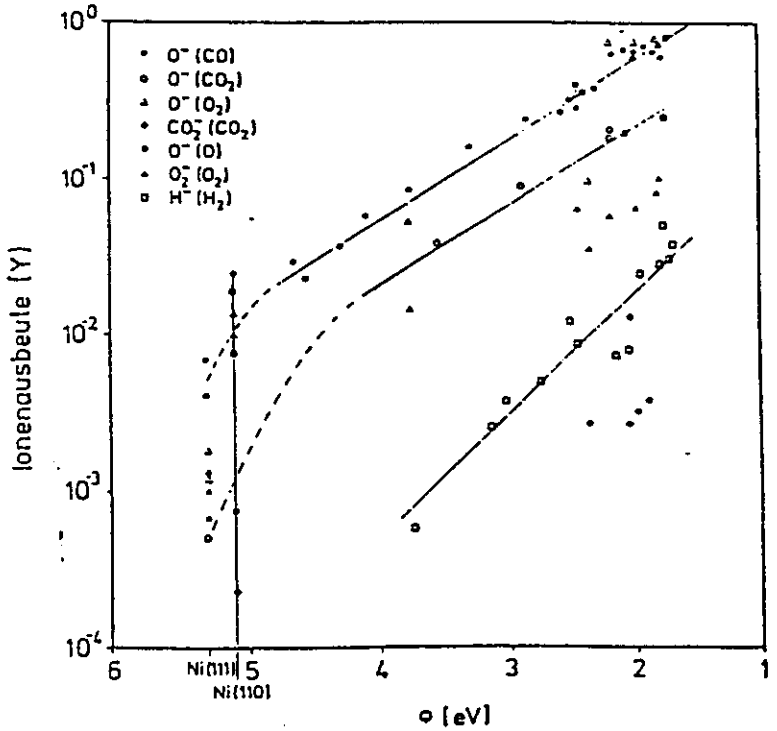

Abb. 21: Die Ionenausbeute als Funktion der Austrittsarbeit der kaliumbedeckten Ni(111)-Oberfläche. Zum Vergleich sind auch die an der Ni(110)-Oberfläche erhaltenen Werte eingezeichnet.

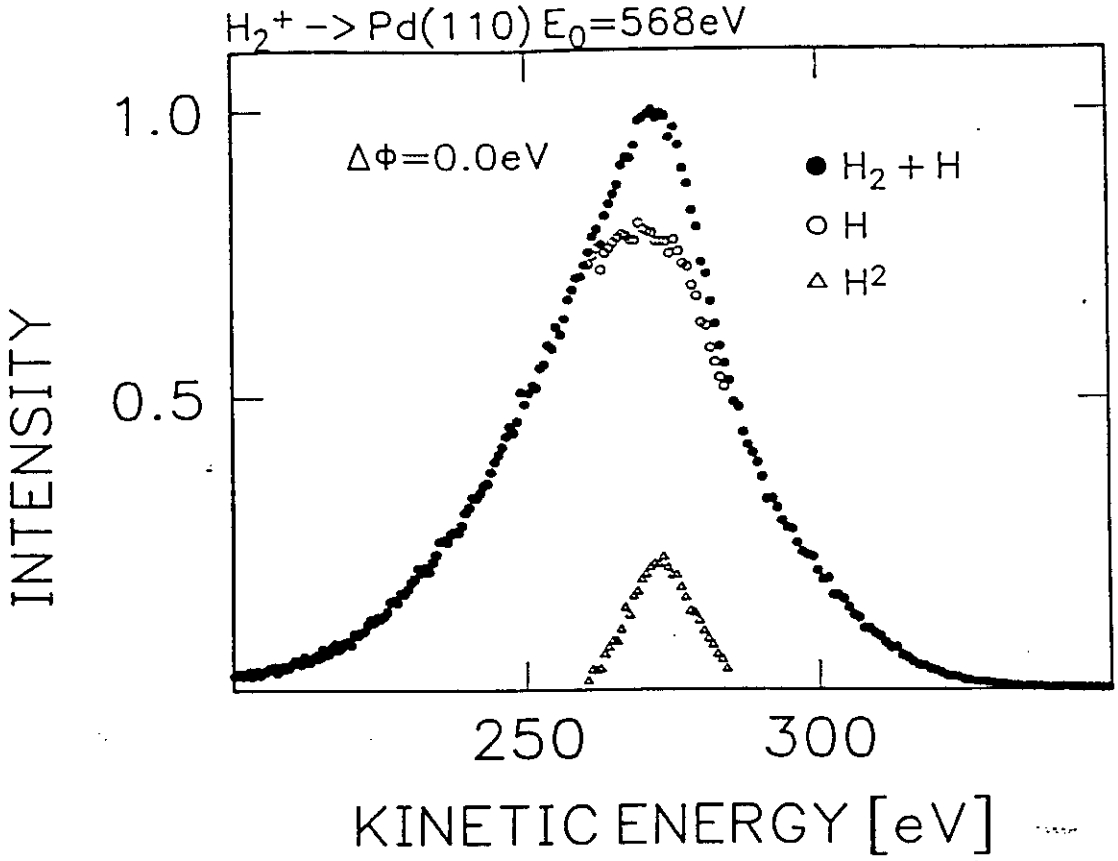
H_2^+ -> Pd(110) E_0=568eV
1.0
0.5
INTENSITY
ΔΦ=0.0eV
● H_2 + H
○ H
△ H^2
250
300
KINETIC ENERGY [eV]

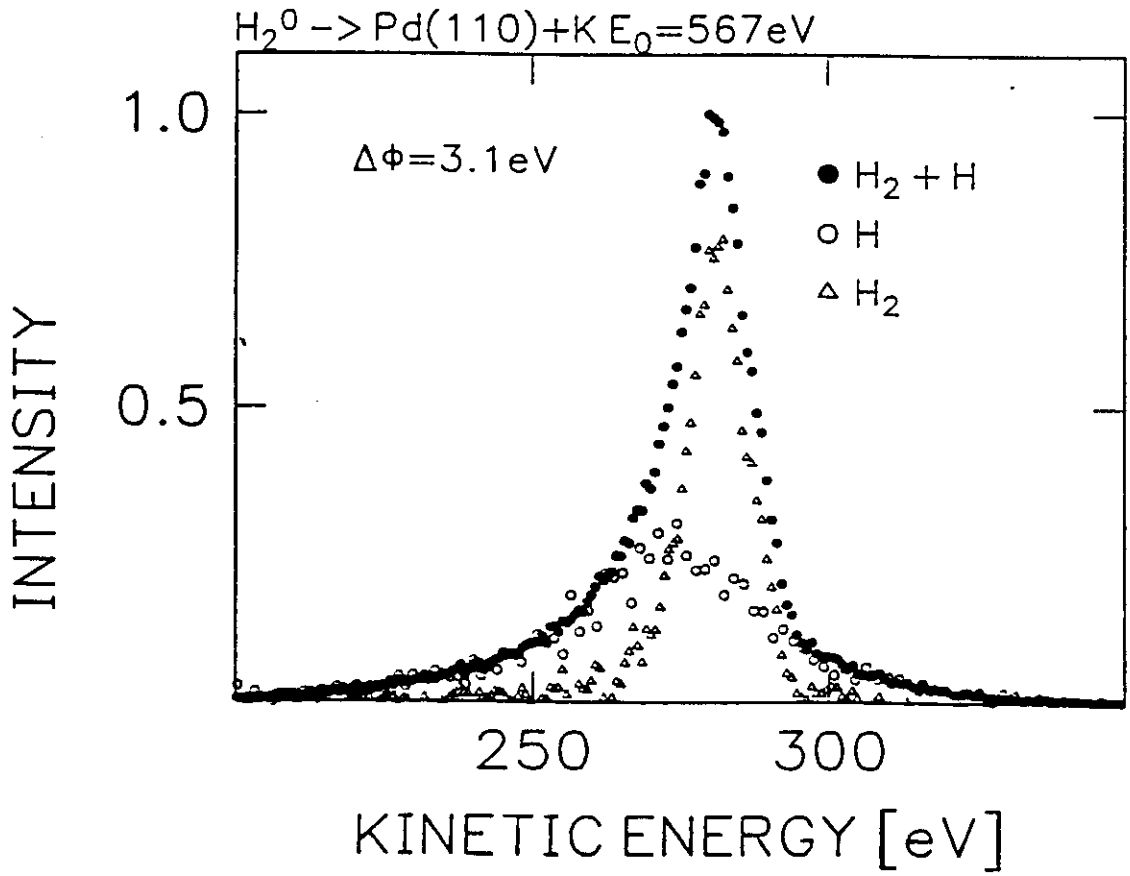
H_2^0 -> Pd(110)+K E_0=567eV
1.0
0.5
INTENSITY
ΔΦ=3.1eV
● H_2 + H
○ H
△ H_2
250
300
KINETIC ENERGY [eV]